# Fate of terrigenous organic matter across the Laptev Sea from the mouth of the Lena River to the deep sea of the Arctic interior

Lisa Bröder [a,b]*, Tommaso Tesi [a,b,c], Joan A. Salvadó [a,b], Igor P. Semiletov [d,e,f], Oleg V. Dudarev [e,f], Örjan Gustafsson [a,b]

[a] *Department of Environmental Science and Analytical Chemistry, Stockholm University, Stockholm, Sweden*

[b] *Bolin Centre for Climate Research, Stockholm University, Stockholm, Sweden*

[c] *Institute of Marine Sciences – National Research Council, Bologna, Italy*

[d] *International Arctic Research Center, University Alaska Fairbanks, Fairbanks, USA*

[e] *Pacific Oceanological Institute, Russian Academy of Sciences, Vladivostok, Russia*

[f] *Tomsk National Research Politechnical University, Tomsk, Russia*

*corresponding author: lisa.broder@aces.su.se

**Abstract**

Ongoing global warming in high latitudes may cause an increasing supply of permafrost-derived organic carbon through both river discharge and coastal erosion to the Arctic shelves. Mobilized permafrost carbon can be either buried in sediments, transported to the deep sea or degraded to $CO_2$ and outgassed, potentially constituting a positive feedback to climate change.

This study aims to assess the fate of terrestrial organic carbon (TerrOC) in the Arctic marine environment by exploring how it changes in concentration, composition and degradation status across the wide Laptev Sea shelf. We analyzed a suite of terrestrial biomarkers as well as source-diagnostic bulk carbon isotopes ($\delta^{13}C$, $\Delta^{14}C$) in surface sediments from a Laptev Sea transect spanning more than 800 km from the Lena River mouth (< 10 m water depth) across the shelf to the slope and rise (2000-3000 m water depth). These data provide a broad view on different TerrOC pools and their behavior during cross-shelf transport. The concentrations of lignin phenols, cutin acids and high-molecular weight (HMW) wax lipids (tracers of vascular plants) decrease by 89-99 % along the transect. Molecular-based degradation proxies for TerrOC (e.g., the carbon preference index of HMW lipids, the HMW acids/alkanes ratio and the acid/aldehyde ratio of lignin phenols) display a trend to more degraded TerrOC with increasing distance from the coast. We infer that the degree of degradation of permafrost-derived TerrOC is a function of the time spent under oxic conditions during protracted cross-shelf transport. Future work should therefore seek to constrain cross-shelf transport times in order to compute a TerrOC degradation rate and thereby help to quantify potential carbon-climate feedbacks.

## 1 Introduction

Amplified global warming in high latitudes has raised growing concern about potential positive carbon-climate feedbacks. Arctic soils store about half of the global soil organic carbon (Tarnocai et al., 2009), with 60 % of this in perennially frozen grounds (Hugelius et al., 2014). With ongoing climate change these vast carbon reservoirs become increasingly vulnerable. Mobilization and transport of old terrigenous organic carbon (TerrOC) into the Arctic Ocean is expected to intensify (Gustafsson et al., 2011) through enhancing river discharge (McClelland et al., 2008) with augmenting sediment loads (Gordeev, 2006; Syvitski, 2002) and accelerating coastal erosion (Günther et al., 2013). This material can be buried in the sediments of the Arctic shelves, transported across the margin towards deeper basins or degraded and re-introduced into the modern carbon cycle as $CO_2$, thereby not only providing a potential positive feedback to global warming, but also causing severe ocean acidification (Semiletov et al., 2016). The fate of permafrost-released TerrOC in the marine environment is thus crucial for future climate projections, yet insufficiently understood (Vonk and Gustafsson, 2013).

The East Siberian Arctic Shelf (ESAS) is with a width of > 800 km the world's largest continental shelf. It receives TerrOC both from the erosion of the East Siberian shoreline, largely consisting of organic-rich, late-Pleistocene ice-complex deposits (Yedoma), and via the Great Russian Arctic Rivers, which drain extensive areas of continuous and discontinuous permafrost. The Laptev Sea is a representative for the TerrOC dominated Siberian shelf seas, since its main organic carbon input originates from substantial coastal erosion (as observed in the Buor-Khaya Bay, Sánchez-García et al., 2011; Semiletov et al., 2011; Vonk et al., 2012) and the Lena River, the main fluvial sediment source for the entire ESAS (Holmes et al., 2002).

Previous studies have focused on near-shore areas and the inner shelf (e.g. Bröder et al., 2016; Charkin et al., 2011; Feng et al., 2015; Karlsson et al., 2011; Salvadó et al., 2015; Sánchez-García et al., 2011; Semiletov et al., 2005, 2012, 2013; Tesi et al., 2014; Vonk et al., 2010, 2012, 2014; Winterfeld et al., 2015b, 2015a). They reported large fractions of old

TerrOC in particulate organic carbon (POC) and surface sediments close to the coast, using different approaches such as applying carbon-isotope-based source apportionment (e.g. Gustafsson et al., 2011; Semiletov et al., 2005; Vonk et al., 2010, 2012, 2014; Salvadó et al., 2015, for the iron-associated OC fraction in the sediment) and by analyzing terrigenous biomarkers in both surface sediments (e.g. Feng et al., 2013; Stein and Macdonald, 2004; Tesi et al., 2014, 2016) and POC in the water column (e.g. Charkin et al., 2011; Karlsson et al., 2011; Winterfeld et al., 2015a). This is the first study that encompasses sampling stations along the entire transect from the Lena River mouth, across the wide Laptev Sea shelf, to the continental slope and rise. Our major objective was to gain new insights regarding the behavior of different TerrOC pools, in particular investigating potential degradation of permafrost-released material along the land-shelf-basin continuum. The Laptev Sea and adjacent East Siberian Sea are among the widest continental margins on Earth (Jakobsson et al., 2004). The resulting long cross-shelf transport and thereby time spent in oxic sediments might exert first order control on TerrOC degradation (e.g. Keil et al., 2004). Our study area is thus well suited to test hypotheses on the fate of permafrost carbon in terms of carbon-climate feedback. We have therefore characterized TerrOC in surface sediments along the Laptev Sea transect on both bulk and molecular level, exploiting source-diagnostic bulk carbon isotopes ($\delta^{13}C$, $\Delta^{14}C$) as well as an extensive biomarker suite (lignin phenols and cutin acids obtained by alkaline CuO oxidation and high-molecular-weight solvent-extractable lipids, such as *n*-alkanes and *n*-alkanoic acids).

## 2 Material and Methods

### 2.1 Study area

The Laptev Sea is the shallowest of the Arctic shelf seas with an average depth of 48 m (Jakobsson et al., 2004). It spans over 498,000 $km^2$ with a volume of 24,000 $km^3$ and is located between the Kara Sea and Severnaya Zemlya in the West and the East Siberian Sea and the New Siberian Islands in the East. The main sources of particulate organic carbon (POC) for the Laptev Sea are terrigenous, both from coastal erosion and river runoff (Sánchez-García et al., 2011; Stein and Macdonald, 2004). Marine primary production is limited to on average two ice-free months per year and therefore generally low. Nutrient-poor waters on the Siberian shelves resulting from a strong stratification further impede phytoplankton growth (Sakshaug, 2004).

The destabilization of Pleistocene Ice-Complex Deposits along the coastline is a main sediment source for the Laptev Sea (Rachold et al., 2000). The total POC input from coastal erosion to Laptev and East Siberian Sea is estimated to be between 4.0 Tg $yr^{-1}$ (Semiletov, 1999; Stein and Fahl, 2000) and 22 ± 8 Tg $yr^{-1}$ (including net subsea permafrost-carbon erosion, Vonk et al., 2012).

The Lena River is estimated to provide 20.7 Tg of sediment per year (Holmes et al., 2002), i.e. > 70 % of the total riverine input to the Laptev Sea (Gordeev, 2006)with an average water discharge of 588 $km^3$ $yr^{-1}$ (Holmes et al., 2012). It drains a watershed of ~2.46 x $10^6$ $km^2$ (Holmes et al., 2012), of which 77 % is underlain by continuous permafrost (Amon et al., 2012). Water discharge peaks in June, during the spring flood, when about 75 % of total organic carbon is delivered (Rachold et al., 2004). Total POC discharge by the Lena River can be up to 0.38 Tg $yr^{-1}$ (Semiletov et al., 2011).

Sediment transport pathways are largely influenced by the prevailing atmospheric conditions: During cyclonic summers (i.e. positive phase of the Arctic Oscillation), northerly winds predominate, strengthening the Siberian Coastal Current, which transports Lena River water masses along the coast towards the East Siberian Sea; whereas during anticyclonic summers (i.e. negative phase of the Arctic Oscillation and mainly southerly winds) the Lena

River plume is exported onto the mid-shelf and towards the deep part of the Arctic Ocean (Charkin et al., 2011; Dmitrenko et al., 2008; Guay et al., 2001; Wegner et al., 2013; Weingartner et al., 1999). Sediment transport in the Laptev Sea is strongly seasonal. The main transport of Lena River water with high concentrations of suspended particulate matter (SPM) towards the mid-shelf takes place shortly after river-ice breakup (Wegner et al., 2005). During the ice-free summer, SPM circulates between inner and mid-shelf with very little material escaping over the shelf break to the deeper parts of the Arctic Ocean. Significant sediment export is suggested to happen during freeze-up through SPM that is incorporated in sea ice and then transported across the continental margin (Dethleff, 2005; Eicken et al., 1997) or through the formation of dense bottom water resulting from brine ejection (Dethleff, 2010; Ivanov and Golovin, 2007). Hardly any sediment transport occurs beneath the ice cover.

Holocene-scale linear sedimentation rates for the Laptev Sea vary between 0.12 and 0.59 mm $yr^{-1}$ according to $^{14}C$ dating of marine bivalves (Stein and Fahl, 2004, and citations therein), whereas centennial-scale $^{210}Pb$-derived rates for the more recent Laptev Sea can be up to 1.3 mm $yr^{-1}$ (Vonk et al., 2012). These rates do not seem to be correlated with water depth on the shelf, but values for the continental slope and rise tend to be on the lower end (0.12-0.38 mm $yr^{-1}$) (Stein and Fahl, 2004, and citations therein).

## 2.2 Sampling

Sediment sampling locations span from close to the Lena River mouth and in the Buor-Khaya Bay, across the shelf, to the continental slope and rise, covering a transect of > 800 km with water depths increasing by more than two orders of magnitude. Samples SW-1, SW-2, SW-3, SW-4, SW-6, SW-14, SW-23 and SW-24 were collected during the SWERUS-C3 expedition on IB *ODEN* during summer 2014 using an Oktopus multicorer (8 Plexiglas tubes, 10 cm diameter). All other samples were collected during the International Siberian Shelf Study (ISSS-08) expedition onboard the RV *Yacob Smirnitskyi* during summer 2008. The YS-4, YS-6, YS-13 and YS-14 samples were taken with a GEMAX gravity corer (2 Plexiglas

tubes, 9 cm diameter); YS-9 and TB-46 were collected with a Van Veen grab sampler. For the grab samples only surface sediments (uppermost cm) were subsampled and used in this study. Sediment cores were cut into 1 cm slices within 24 hours after sampling. To account for lower sediment accumulation rates on the rise, for SW-1, SW-2, SW-3 and SW-4 a higher resolution of 0.5 cm for the top 10 cm was chosen. The depositional age for all samples is thus between ~8 and ~70 years (depending on which sedimentation rates are employed). All samples were kept frozen throughout the expedition and freeze-dried upon arrival to Stockholm University laboratories. See Semiletov and Gustafsson (2009) for more information on the ISSS-08 expedition. For exact sampling locations see Table 1.

## 2.3 Surface area

All surface area analyses have been performed on a Micromeritics Gemini VII Surface Area and Porosity analyzer. Freeze-dried subsamples of ~0.7 g were furnaced at 400 °C for 12 h and gently cooled down to room temperature to remove all organic material. Keil and Cowie (1999) have shown that this method yields statistically similar results to the method using removal with sodium pyrophosphate/ hydrogen peroxide (Mayer, 1994). The samples were then desalted by repeated mixing with 50 ml of MilliQ water and centrifugation (20 min at 8000 rpm), followed by further freeze-drying. Directly prior to analysis they were degassed in a Micromeritics FlowPrep 060 Sample Degas System for 2 h at 200 °C under a constant nitrogen flow. Each analysis was initiated by measuring the free space in the vial. The specific surface areas were derived from 6 pressure-point measurements (relative pressure p/p0 = 0.05-0.3, equilibration time 5 s) with nitrogen as adsorbing gas (Brunauer et al., 1938). The instrumental precision was 0.1-0.3 $m^2 g^{-1}$, which corresponds to a relative uncertainty of about 1 %. The performance of the instrument was monitored with the surface area reference material Carbon Black (21.0 ± 0.75 $m^2 g^{-1}$) provided by Micromeritics.

## 2.4 X-Ray Fluorescence

The mineral composition of ~1 g freeze-dried, homogenized subsamples was also characterized with a wavelength dispersive sequential Philips PW2400 X-ray Fluorescence (XRF) spectrometer. Prior to the analysis, sediment samples were combusted for 12h at 450 °C to remove the organic fraction. The XRF was operated under vacuum conditions on samples prepared as glass beads using lithium tetraborate and melted with a fluxer Claisse Fluxy (~1150°C) (Mercone et al., 2001). The relative error was less than 0.6 % for major elements and less than 3 % for trace elements. In this study only $SiO_2$, $Al_2O_3$ and CaO are reported.

## 2.5 Bulk elemental and carbon isotope analysis

Concentration and $\delta^{13}C$ isotopic composition of total organic carbon (TOC) were determined at the Stable Isotope Laboratory, Department of Geological Sciences, Stockholm University. Homogenized subsamples of ~10 mg were repeatedly acidified (HCl,1.5 M, Ag capsules) to remove carbonates (Nieuwenhuize et al., 1994). TOC concentrations and $\delta^{13}C$ isotopic composition were measured simultaneously with a Carlo Erba NC2500 elemental analyzer connected via a split interface to a Finnigan MAT Delta V mass spectrometer. TOC concentrations were blank corrected and the relative error was < 1 %. Stable isotope data are reported relative to VPDB using the $\delta^{13}C$ notation.

Radiocarbon analyses of acidified samples were conducted at the US National Ocean Sciences Accelerator Mass Spectrometry (NOSAMS) Facility of the Woods Hole Oceanographic Institution, USA, according to their standard routines (Pearson et al., 1998). The relative error of the measurements was < 0.5 %. Radiocarbon data are reported using the $\Delta^{14}C$ notation following Stuvier and Polach (1977).

## 2.6 Biomarkers

### 2.6.1 CuO-oxidation products

Microwave-assisted alkaline CuO oxidation was performed according to the method established by Goñi and Montgomery (2000). Homogenized subsamples of 100-400 mg of

sediment (corresponding to 2-5 mg OC) were combined with 300 mg of copper(II) oxide and 50 mg of ferrous ammonium sulfate and oxidized under oxygen-free conditions (degassed NaOH, 8 wt %) at 150 °C for 90 min using an UltraWAVE Milestone 215 Microwave oven. After oxidation, known amounts of trans-cinnamic acid and ethyl vanillin were added as recovery standards. Samples were acidified to pH 1 with HCl (12 M) and repeatedly extracted with ethyl acetate. Anhydrous $Na_2SO_4$ was added to remove remaining water. The solvent was evaporated and extracts re-dissolved in pyridine. For quantification, subsamples were derivatized with bis-trimethylsilyl-trifluoroacetamide (BSTFA) + 1 % trimethylchlorosilane (TMCS) and analyzed on a gas-chromatograph mass spectrometer in full scan mode (GC-MS, Agilent) using a DB5-MS capillary column (60 m x 250 µm, 0.25 µm stationary phase thickness, Agilent J&W) with a temperature profile of initially 60 °C followed by a ramp of 5 °C $min^{-1}$ until reaching and holding 300 °C for 5 min. The quantification of lignin phenols, benzoic acids, and p-hydroxybenzenes was achieved by comparison to the response factors (key ions) of commercially available standards. For cutin-derived products, fatty acids and dicarboxylic acids the response factor of trans-cinnamic acid was used as in Goñi et al. (1998).

### 2.6.2 Solvent-extractable lipids

Wax lipids were extracted by means of accelerated solvent extraction (Dionex ASE 300) using dichloromethane:methanol (9:1) according to the method described by Wiesenberg et al. (2004). Pre-rinsed stainless-steel vessels were loaded with ~3 g of freeze-dried sediment, filled up with pre-combusted glass beads and pre-combusted glass fiber filters at both ends. Two extraction cycles were performed per sample applying a static pressure of 1500 psi and a temperature of 80 °C for 5 min after a heating phase of 5 min. The flush volume was 50 % of the 34 ml cell size with a purging time of 100 s.

Extracts were further purified (addition of activated Cu for sulfur and anhydrous $Na_2SO_4$ for water removal) and then separated into a neutral and an acid fraction using BondElut cartridges (bonded phase $NH_2$, Varian), eluting with dichloromethane:isopropanol (2:1) for

223 the neutral and methyl *tert*-butyl ether with 4 % acetic acid for the acid fraction according to
224 the method described by van Dongen et al. (2008a). The neutral fraction was further
225 separated into a polar and a non-polar fraction with an $Al_2O_3$ column. For each of the three
226 compound classes *n*-alkanes (neutral non-polar fraction), *n*-alkanols (neutral polar fraction)
227 and *n*-alkanoic acids (acid fraction) ~10 mg of one internal standard, $d_{50}$-tetracosane, 2-
228 hexadecanol and $d_{39}$-eicosanoic acid respectively, were added to the sediment samples prior
229 to extraction. All fractions were then analyzed on a GC–MS (Agilent) using the same column
230 and temperature program as for the CuO products. The polar and acid fractions were
231 derivatized with BSTFA + 1 % TMCS prior to analysis. Quantification was performed using a
232 5-point calibration curve with commercially available standards. Here, we only report data for
233 high-molecular weight (HMW) *n*-alkanes and *n*-alkanoic acids, where HMW refers to carbon
234 chain-lengths of ≥ 23 for *n*-alkanes and ≥ 24 for *n*-alkanoic acids.

## 3 Results and Discussion

The fate of permafrost-released terrigenous organic carbon (TerrOC) across the Laptev Sea shelf is controlled by competing processes. Degradation and sorting, as well as replacement of TerrOC by autochthonous marine organic matter all co-occur to varying degrees during cross-shelf transport. To disentangle their effects on the fate of permafrost-released TerrOC we first report changes in bulk sediment and OC properties and then focus on differences on the molecular level.

### 3.1 Characterization of the transect on a bulk level

Bulk total organic carbon (TOC) concentrations decreased across the shelf with highest values (~2 %) at shallow water depths and lowest values on the shelf edge (~0.8 %); at high water depths (> 2000 m) concentrations were slightly higher (~1 %). TOC values and the general pattern were in accordance with previous data from the Laptev Sea (Semiletov et al., 2005; Shakhova et al., 2015; Stein and Fahl, 2004; Vonk et al., 2012) and within the same range of those measured for the North American Arctic margin (Goni et al., 2013).

Normalizing TOC concentrations to the mineral-specific surface area (SA) helps to understand the influence of physical sorting and preferential deposition on the observed TOC trends since SA is correlated to the sediment grain size to a first order approximation. To test if the mineral surface area is altered by the input of autochthonous organisms with siliceous or carbonaceous skeleton (e.g. silicoflagellates/diatoms or foraminifera/shells respectively), the mineral composition of the sediments was examined by X-ray fluorescence analysis. There were no apparent trends with water depth for either $SiO_2/Al_2O_3$ or $CaO/Al_2O_3$; therefore, marine production is not expected to have a measureable effect and SA can thus be regarded as a conservative parameter. This was also confirmed by low biogenic silica concentrations for the Laptev Sea reported earlier (< 1.4 %, Mammone, 1998).

The relationship between TOC and SA has been widely studied on continental margins (e.g. Blair and Aller, 2012; Keil et al., 1994; Mayer, 1994). The TOC/SA ratios of typical river suspended sediments range between 0.4 and 1 mg $m^{-2}$ (Mayer, 1994). TOC/SA ratios > 1

mg $m^{-2}$ have been found in areas with high TOC supply (e.g. river outlets) and where the deposited organic matter had spent little time under oxic conditions (short oxygen exposure time, OET) (Mayer et al., 2002). Ratios < 0.4 mg $m^{-2}$ generally correspond to sediments from deeper parts of the ocean and long OETs (e.g. Aller and Blair, 2006). Accordingly, the TOC/SA values along the Laptev Sea transect displayed a strong decrease from 2.2 and 1.7 mg $m^{-2}$ close to the Lena River delta (water depths of 11 and 7 m, respectively) to about 0.3 mg $m^{-2}$ at water depths greater than 2000 m (Fig. 2A), proposing extensive TOC loss during cross-shelf transport.

Bulk TOC isotopes have been broadly used to distinguish between organic matter sources. Radiocarbon isotopes ($^{14}C$) convey information about the age of organic material, with younger OC having higher $\Delta^{14}C$ values. Marine organic matter produced primarily from $CO_2$ is expected to have modern $^{14}C$ signatures, whereas permafrost-derived TerrOC has aged both on land and during transport and has thus more depleted $^{14}C$ values. The $\Delta^{14}C$ values for our Laptev Sea transect were generally low (< -280 ‰, Fig. 2B), suggesting a significant input of pre-aged TerrOC (as in Vonk et al., 2012). Bulk TOC showed less depleted $\Delta^{14}C$ signatures with increasing distance from land on the shelf (from about -500 ‰ to about -340 ‰ on the outer shelf, Fig. 2B), reflecting a dilution of older TerrOC with younger marine material. On the slope and rise, however, $\Delta^{14}C$ values decreased again to about -410 ‰. This difference may be a result of ageing during lateral transport and/or after deposition due to lower accumulation rates on slope and rise. The range between -340 ‰ and -410 ‰ corresponds to a $\Delta^{14}C$ age difference of about 900 years; however, the depositional age differences between shelf and slope samples were estimated to be less than 80 years (see Section 2.2). Ageing after burial alone does therefore not explain the difference in $\Delta^{14}C$. Keil et al. (2004) estimated a lateral transport time of 1800 years across the Washington margin (158 km) from $\Delta^{14}C$ data of bulk OC in surface sediments. For the > 200 km distance between mid-shelf and rise a bulk ageing of 900 years does therefore not seem unreasonable. It has to be taken into account, however, that mainly the TerrOC fraction of the bulk OC is subject to such protracted lateral transport. Transport times would thus have

291 to be significantly higher in order to explain this age difference for the entire bulk OC. One
292 indication supporting this hypothesis of protracted lateral transport of TerrOC is the
293 degradation status of TerrOC at the deep stations. All molecular degradation proxies point
294 towards highly reworked material (see Section 3.3), suggesting that only the most refractory
295 TerrOC fraction is found at great water depths off the continental margin. Alternatively, the
296 lower $\Delta^{14}C$ values at high water depths may be the consequence of more effective
297 degradation of marine organic matter throughout the water column, resulting in a
298 comparatively lower input of young autochthonous material. However, this latter scenario is
299 not supported by the stable carbon isotopic signature.
300 For stable carbon isotopes ($^{13}C$), terrigenous sources are generally more depleted than
301 marine organic matter (Fry and Sherr, 1984). In this study, values for $\delta^{13}C$ of TOC ranged
302 between -26.5 ‰ and -22.3 ‰. The trend towards more enriched TOC with increasing
303 distance from the coast (Fig. 2B) can be explained by a growing proportion of marine organic
304 matter. However, the $\delta^{13}C$ signature of the marine source appeared to be heavier than typical
305 marine planktonic material in that region (-26.7 ± 1.2 ‰, Panova et al., 2015; -24 ± 3 ‰,
306 Vonk et al., 2012, and citations therein). One possible explanation for this discrepancy is an
307 underestimated influence of ice algae that were reported to have highly enriched $\delta^{13}C$ values
308 between -15 to -18 ‰ (Schubert and Calvert, 2001). Significant seafloor deposition of ice
309 algal biomass has been observed previously for the Arctic basins (Boetius et al., 2013).
310 Another option would be a more refractory, isotopically-enriched marine endmember (-21.2
311 ‰) as suggested by Magen et al. (2010). They argue that lighter isotopes are preferentially
312 consumed by bacteria, which in turn enriches the remaining marine organic matter. Following
313 their reasoning, the more enriched values observed for this transect may be interpreted as
314 an increasing proportion of refractory marine organic matter.
315 Winterfeld et al. (2015b) analyzed surface water particulate organic carbon (POC) in the
316 Lena River delta and found a mean $\delta^{13}C$ of -29.6 ± 1.5 ‰. Karlsson et al. (2011) reported
317 similarly depleted $\delta^{13}C$ values for POC from the Buor-Khaya Bay (-29.0 ± 2.0 ‰), while their
318 mean value for sedimentary OC for the same stations was significantly more enriched (-25.9

± 0.4 ‰) and agreed well with our data for the shallow stations (-26.2 ± 0.3 ‰, stations YS-13, YS-14 and TB-46). Lena River POC $\delta^{13}C$ values from high-discharge periods agree well with the more enriched values we found for the shallow stations (Rachold and Hubberten, 1998). Stein and Fahl (2004), Semiletov et al. (2011, 2012) and Vonk et al. (2012) presented similar $\delta^{13}C$ ranges and trends for sediments from parts of the Laptev Sea as is reported in the current study for the entire width of the Laptev Sea shelf. For the Arctic Amerasian Continental shelf, Naidu et al. (2000) reported contrasts in absolute $\delta^{13}C$ values comparing surface sediment samples from different regions, but all commonly displayed an increasing trend for $\delta^{13}C$ values across the shelf, suggesting a growing fraction of marine organic matter with increasing distance from the coast.

Combining TOC/SA ratios with stable isotope signatures ($\delta^{13}C$) may serve to disentangle two different processes, which occur synchronously during cross-shelf transport (as in Keil et al. 1997a): 1.) The net loss of TerrOC and 2.) the replacement of TerrOC with autochthonous marine OC. Net loss of TerrOC, caused by either degradation or hydrodynamic sorting during transport, has been quantified previously using TOC/SA ratios (e.g. Aller and Blair, 2006; Keil et al., 1997a). The carrying-capacity of inorganic particles for OC is assumed to be a function of the SA (Mayer, 1994); a decrease in TOC/SA values can therefore be regarded as TOC net loss.

Replacement of TerrOC with autochthonous marine OC does not change this ratio. But since marine OC is known to be isotopically enriched in $\delta^{13}C$ over TerrOC, this process is recorded by an increasing isotopic signature. Along the Laptev Sea transect, both processes seemed to play an important role (Fig. 2C). High TOC/SA values close to the Lena River decreased sharply outbound in the nearshore regime, pointing to extensive net loss, while the increase in $\delta^{13}C$ values was minor in this area. Once TOC/SA ratios were < 0.8 mg $m^{-2}$ (water depths > 20 m), the isotopic changes and thus the replacement of TerrOC with marine OC became increasingly important. Similar trends were observed for the Amazon River delta (Keil et al., 1997b).

However, the TOC/SA trend in the shallower sediments is likely driven by both degradation of OC bound to the mineral matrix during cross-shelf transport and sorting of vascular plant fragments that are retained in the inner shelf. A recent study (Tesi et al., 2016) has shown that ~50 % of the total OC pool in the inner Laptev shelf surface sediments exists in the form of large vascular plant fragments. They are trapped close to the coast due to their size and resulting settling (Stoke's law), while the OC bound to the fine mineral matrix is more buoyant and transported offshore towards deeper waters.

## 3.2 Molecular indicators of organic matter sources

### 3.2.1 Biomarker distributions

The abundances of different source-diagnostic molecular proxies have been extensively investigated to elucidate complex carbon-cycling mechanisms. In this study, a biomarker suite of CuO oxidation products and solvent-extractable lipids was analyzed in order to gain more insights on TerrOC sources and degradation status along the Laptev Sea transect. All biomarker concentrations were normalized to the sediment-specific surface area (SA) instead of OC content to avoid the signals being overshadowed by other carbon pools. As shown by the lack of water-depth-related changes in the mineral composition (Section 3.1), mineral-matrix dilution by biogenic material is negligible.

Lignin-derived phenols have been widely used to trace TerrOC in the marine environment (e.g. Ertel and Hedges, 1984; Goñi and Hedges, 1995; Hedges and Mann, 1979). The lignin macro-molecule is only synthesized in vascular plants (and certain seaweed species that are not existing in the study area) to render stability to the cell walls. Lignin-derived phenols are typically grouped by phenol type (V: vanillyl phenols, i.e. vanillin, acetovanillone, and vanillic acid; S: syringyl phenols, i.e. syringaldehyde, aceto syringone, and syringic acid; C: cinnamyl phenols, i.e. p-coumaric and ferulic acids). Total lignin refers to the sum of the three groups. Across the shelf, lignin loadings decreased substantially with increasing distance from the coast/water depth (45 μg $m^{-2}$ close to the coast, 0.43 ± 0.09 μg $m^{-2}$ for the deep stations; loss of 99.1 ± 0.2 %, Fig. 3A).

374 Cutin-derived hydroxy fatty acids are another compound class obtained from CuO oxidation,
375 which have been used in parallel with lignin phenols (e.g. Goñi et al., 2000; Prahl et al.,
376 1994). They are mainly associated with the soft tissues of vascular plants such as leaves and
377 needles. Cutin acid loadings displayed a similar trend as lignin phenols (11 μg $m^{-2}$ close to
378 the coast, 0.061 ± 0.010 μg $m^{-2}$ for the deep stations; loss of 99.4 ± 0.1 %, Fig. 3A).
379 Similar values and sharp declines with increasing distance from the coast for lignin and cutin
380 have been observed for the whole East Siberian Arctic Shelf (ESAS) (Tesi et al., 2014) (Fig.
381 4 for comparison of lignin phenol concentrations with literature values for different Arctic
382 margins). A recent study (Winterfeld et al., 2015a) for the Buor-Khaya Bay (5.8-17 m water
383 depth) reported lignin phenol concentrations on the same order of magnitude, up to 40 %
384 higher for the shallowest samples, and decreasing with increasing depth. For the Beaufort
385 Sea shelf, Goñi et al. (2000) found a less drastic decline in lignin phenols and cutin acids
386 going from 5 m water depth to 210 m, which likely reflected both lower concentrations in the
387 shallow waters (factor of ~2), and a narrower and steeper shelf. Lignin phenols were also
388 higher at greater water depths than on the ESAS. This may reflect the differences in
389 bathymetry: since the Beaufort Sea shelf is not as wide as, but steeper than, the ESAS,
390 lateral transport is possibly faster, leaving less time for organic matter to be degraded along
391 the way. A comparison between different shelf-slope systems across the North American
392 Arctic margin (Goni et al., 2013) revealed very low lignin and cutin concentrations for the
393 Canadian Archipelago, Lancaster Sound and Davis Strait, whereas both concentrations and
394 trends with water depth for the Beaufort Sea, Chuckchi Sea and Bering Sea were similar to
395 the results from this study. An exception to these patterns was Barrow Canyon, where at
396 water depths of > 2000 m lignin and cutin concentrations were as high as the ones observed
397 close to the Lena River delta, pointing to efficient rapid TerrOC transfer with comparably
398 short oxygen exposure times through this active canyon (Goni et al., 2013) (Fig. 4 and Fig.
399 S1).
400 Solvent extractable high-molecular weight (HMW) *n*-alkanes and *n*-alkanoic acids make up
401 the major part of epicuticular leaf waxes (Eglinton and Hamilton, 1967) and have been

broadly employed as TerrOC biomarkers (for the Arctic Ocean e.g. van Dongen et al., 2008; Yunker et al., 1995, 2005). HMW wax lipids in this study also presented a decreasing trend with increasing water depth/distance from the coast, but to a lesser extent than lignin phenols or cutin acids (HMW *n*-alkanes: 1.1 µg $m^{-2}$ close to the coast, 0.12 ± 0.02 µg $m^{-2}$ for the deep stations; HMW *n*-alkanoic acids: 12 µg $m^{-2}$ close to the coast, 0.42 ± 0.29 µg $m^{-2}$ for the deep stations; loss of 89 ± 2 % and 96 ± 3 %, respectively, Fig. 3B).

Previous studies in the same area reported similar lipid biomarkers concentrations, which confirm the magnitude of the decreasing trends with increasing water depth (Karlsson et al., 2011; Vonk et al., 2010) (Fig. S1). HMW *n*-alkane concentrations in the Beaufort and the Chuckchi Sea (Belicka et al., 2004; Yunker et al., 1993) are in accordance with the ones measured on the ESAS, but the shallowest sample on the Beaufort Shelf is ~2 times lower than the shallow ESAS samples (Fig. S1). This might imply that sediments transported by the Mackenzie River to the Beaufort Shelf have lower TerrOC concentrations than Lena River transported sediments. For the Mackenzie Shelf, Goñi et al. (2000) used lignin phenols and cutin acids to estimate a terrigenous $\delta^{13}C$ endmember and therewith derived a terrigenous contribution of almost 80 % for the shallowest sediments, while rough estimates from C/N and $\delta^{13}C$ data suggested that TerrOC made up only 30-50 % of the organic carbon (Macdonald et al., 2004). For the Lena Delta, source apportionment calculations using $\delta^{13}C$ and $\Delta^{14}C$ data attributed up to 83 % of the organic carbon to terrigenous sources (Vonk et al., 2012).

All TerrOC biomarker loadings displayed a strong decrease across the shelf, but their relative losses differ substantially between compound classes (Fig. 3C). These findings agree with previous results for the ESAS (Tesi et al., 2014), where similar differences between biomarkers were reported. A somewhat larger decrease was observed for lignin than for cutin, in contrast to this study. The different extents of biomarker losses for the different compound classes may either be attributed to preferential degradation of lignin phenols and cutin acids, implying that they are more labile than HMW *n*-alkanes and *n*-alkanoic acids, or sorting during transport, suggesting that they are associated with a sediment fraction that is

hydraulically more retained and carried less efficiently to the outer shelf/slope. A recent study (Tesi et al., 2016) aimed to disentangle these two processes by analyzing different fractions of bulk surface sediments from three transects (yet with only three stations each) acrossthe ESAS. The fractions were separated according to density (1.8 g $cm^{-3}$ cutoff), size (>63 µm, 38-63 µm, < 38 µm) and settling velocity (1 m $d^{-1}$ cutoff). The highest lignin phenol abundance was found in low-density plant fragments (26-55 mg $g^{-1}$ OC). These large particles have a higher settling velocity (Stokes' law) and are therefore hydraulically retained close to the coast. Cutin acids and plant wax lipids were mainly associated with the high-density fine (< 38 µm, > 1 m $d^{-1}$) and ultrafine (< 38 µm, < 1 m $d^{-1}$) mineral fractions. Within the fine and ultrafine fractions, which made up about 95 % of the organic carbon on the outer shelf, they found drastic losses of all biomarkers with increasing distance from the coast, which they attributed to degradation during the protracted cross-shelf transport. Relative decreases appeared to depend on the number of functional groups of the compound class: 98 ± 1 % for lignin phenols, 97 ± 1 % for cutin acids, 96 ± 1 % for HMW *n*-alkanoic acids and 89 ± 4 % for HMW *n*-alkanes. According to that study, the steep cross-shelf gradients observed here for lignin phenols can be attributed to both hydrodynamic sorting close to the coast and degradation during transport. From the data in the current study alone, the two processes occurring in parallel - degradation and sorting during cross-shelf transport - cannot be disentangled. However, using the data from (Tesi et al., 2016), we can make a rough correction for the sorting part to derive an estimate of the net extent of degradation. For the shallowest station in their study (same as here, TB-46), about 75 % of the lignin phenols were associated with the low density fraction that was retained close to the coast. If we thus assume only 25 %, i.e. 11 of the 45 µg $m^{-2}$ to be associated with the fine fraction that is actually transported across the shelf, we obtain a reduction by 96 ± 1 % that can be attributed to degradation (compared to 99.1 % net loss). These results agree with the values presented in (Tesi et al., 2016). For the other compounds analyzed 55-74 % are associated with the fine fraction even for the shallowest station and they therefore experience sorting to a lesser extent.

458 Degradation after burial is assumed to play only a minor role. Differences in sedimentation
459 ages are expected to be small (Section 2.1) and a study on centennial-scale sediment cores
460 from the East Siberian Sea (Bröder et al., 2016) detected no significant TerrOC degradation
461 (as recorded by biomarker loss) with increasing sediment depth. Also in that study, lignin
462 phenol and cutin acid loadings were on average 20 times higher on the inner than on the
463 outer shelf, whereas for HMW *n*-alkanoic acids and *n*-alkanes the difference between inner
464 and outer shelf was only a factor of ~3-5. Contrasts between the stations were found to be
465 larger than down-core changes. This may be due to the fact that the cores in that study only
466 encompassed about one century of sedimentation ages, while the protracted cross-shelf
467 transport likely requires much longer timescales.
468
469 3.2.2 Lignin Phenol sources
470 Relative distributions of different lignin phenol classes reveal more information on TerrOC
471 sources since they are specific to different plant types. Syringyl phenols are not produced by
472 gymnosperm (non-flowering) plants; elevated syringyl to vanillyl ratios (i.e. S/V > 1, Hedges
473 and Parker, 1976) are therefore attributed to more lignin phenols from angiosperm
474 (flowering) plants. These ratios have to be handled with care, though, because the
475 preferential degradation of syringyl phenols by white- and brown-rot fungi on land can also
476 alter S/V ratios (Hedges et al., 1988). S/V values for the Laptev Sea transect increased with
477 increasing water depth from ~0.65 for the inner shelf to ~1.0 for the slope/rise sediments
478 (Fig. 5A). This trend can either be explained by preferential degradation of gymnosperm
479 material or sorting during transport. Tesi et al. (2014) measured generally lower values for
480 S/V (ESAS average: 0.47, for only Lena watershed dominated locations: 0.42) recording no
481 trend with water depth (Fig. S1 for comparisons with other studies). Their deepest station
482 was located at only 69 m water depth, though, whereas in this study sediments from down to
483 3146 m water depth were analyzed. S/V ratios in Buor-Khaya Bay surface sediments
484 (Winterfeld et al., 2015a) were also lower (0.43 ± 0.02 on average) and displayed no trend
485 with water depth. Within the water depth interval they studied (5.8-17 m), however, the

samples analyzed in this study had also quite homogeneous S/V ratios (0.64 ± 0.02). Two sediment cores from the East Siberian Sea (Bröder et al., 2016) showed also lower S/V values (inner shelf surface sediment: 0.62, outer shelf surface sediment: 0.50) displaying no clear trends over time/down-core. For the Beaufort Sea shelf Goñi et al. (2000) detected rather high values (0.54-1.71), which (besides the very high value at 61 m water depth) agree with the data from this study. Other transects across the North American Arctic margin (Goni et al., 2013) had slightly lower S/V ratios with no observed trends with water depth.

The ratio of cinnamyl to vanillyl phenols (C/V) is associated with the relative contributions of woody versus soft material, because only non-woody vascular plants synthesize cinnamyl phenols (Hedges and Mann, 1979a). This ratio admittedly decreases with ongoing degradation (Opsahl and Benner, 1995) and may therefore not be used as an unambiguous source indicator. We observed that C/V values strongly decreased across the Laptev Sea Shelf from ~0.5 (close to the Lena River outlet) to ~0.1 (on the slope/rise, Fig. 5B), which may reflect the preferential degradation of soft tissues. This trend is not likely caused by hydrodynamic sorting, since typically the larger, low-density, woody plant fragments are retained in shallower water, whereas finer material is transported further across the shelf (e.g. Keil et al., 1994; Tesi et al., 2016).

C/V ratios in Buor-Khaya Bay sediments (Winterfeld et al., 2015a) in shallow waters were on average lower and more homogeneous (0.17 ± 0.03) than those measured in this study (0.41 ± 0.12 for the corresponding depth interval) (Fig. S1 for comparisons with other studies). C/V values for the entire ESAS were on average 0.15 (0.14 ± 0.07 for only Lena dominated waters) with no water depth trend (Tesi et al., 2014). In shallow sediment cores from the East Siberian Sea, Bröder et al. (2016) measured C/V ratios of 0.20 (inner shelf) and 0.13 (outer shelf) for the surface sediments with no significant trend over sediment depth. For the Mackenzie Shelf C/V values ranged between 0.16 and 0.32 and slightly increased with increasing water depth (Goñi et al., 2000). In contrast, in the Bering Sea, Chuckchi Sea, Barrow Canyon, Canadian Archipelago, Lancaster sound and Davis Strait there were no C/V trends observed (Goni et al., 2013), with lower values in the Canadian part (0.10 ± 0.12) and

highest values on the Beaufort Sea slope, where values slightly decreased with increasing depth (0.39 ± 0.07).

A comparison to the S/V-C/V signatures of potential Arctic plant end-members (compiled by Amon et al., 2012, and citations therein, Tesi et al., 2014, and Winterfeld et al., 2015a) showed that lignin phenols likely derive from both angio- and gymnosperm soft tissues in the shallower samples, closely matching with willow (*Salix*) tissues measured by Winterfeld et al. (2015a). With increasing water depths, angiosperm wood became the most important source material, while gymnosperm wood, grasses and mosses did not appear to contribute significantly to the overall lignin phenol fingerprint (Fig. 5C). As discussed earlier, this trend may well be a result of preferential degradation and sorting during cross-shelf transport and not derive from actual changes in source material.

### 3.3 Degradation status of organic matter

During degradation, syringyl and vanillyl phenol aldehydes are oxidized to carboxylic acids of the same phenol group. Increasing Sd/Sl and Vd/Vl ratios can therefore qualitatively indicate ongoing degradation of lignin phenols (Ertel and Hedges, 1984; Hedges et al., 1988). For fresh plant material typical acid-to-aldehyde ratios are around 0.1-0.2 (Hedges et al., 1988). Winterfeld et al. (2015a), however, found values as high as Sd/Sl = 0.80 and Vd/Vl = 0.67 for a moss species (*Aulacomnium turgidum*), Sd/Sl = 0.87 for larch (*Larix*) needles and Sd/Sl = 0.49 Vd/Vl = 0.41 for wild rosemary (*Ledum palustre*). Sedges (*Carex spp.*), dwarf birch (*Betula nana*) and willow (*Salix*) range between Sd/Sl = 0.13-0.24 and Vd/Vl = 0.18-0.23. The ratio of CuO oxidation-derived 3,5-dihydroxybenzoic acid to vanillyl phenols (3,5-Bd/V) also serves as a proxy for degradation as 3,5-Bd is formed during humification likely occurring in soils (Gordon and Goñi, 2004; Hedges et al., 1988; Prahl et al., 1994; Tesi et al., 2014). For this reason, this proxy can trace mineral rich soil organic matter in contrast to vascular plant debris (e.g. Dickens et al., 2007; Prahl et al., 1994) as well as degradation during cross shelf transport (Tesi et al., 2016).

Sd/Sl, Vd/Vl and 3,5-Bd/V all increased along the transect, implying more degraded material with increasing residence time in the shelf system (Fig. 6A). There appeared to be no differences between outer shelf/slope and rise, which may indicate that TerrOC on the slope is already highly reworked. In contrast, Tesi et al. (2014) found no correlation between Sd/Sl or Vd/Vl and distance from the coast, while 3,5-Bd/V significantly increased with increasing distance from the coast (Fig. S2 for comparisons with other studies). Sd/Sl values for the Buor-Khaya Bay from Winterfeld et al. (2015a) were slightly higher (1.04 ± 0.24) than samples from the corresponding water depths in this study (0.66 ± 0.15), whereas Vd/Vl values were significantly higher (1.28 ± 0.30 compared to 0.59 ± 0.14). Measurements for the Mackenzie Shelf agreed with the ones in this study (Sd/Sl = 0.81 ± 0.25 compared to 1.01 ± 0.33 for the corresponding water depths; Vd/Vl = 0.69 ± 0.14 to 0.86 ± 0.26; 3,5-Bd/V = 0.19 ± 0.04 to 0.31 ± 0.15), but did not show a trend with water depth (Goñi et al., 2000).

Tesi et al. (2016) observed lower acid/aldehyde ratios for the lignin-rich low-density fraction compared to the other fractions (high-density with different grain sizes and settling velocities) in coastal surface sediments from the ESAS. With increasing distance from the coast, these values increased, whereas for the other fractions there were no apparent trends. These findings were interpreted as relatively fresh lignin in the low-density fraction (rich in large plant fragments) compared to the relatively degraded lignin that had likely experienced leaching and adsorbed to the fine mineral fractions (i.e. mineral bound OC). Bulk 3,5-Bd/V values are potentially affected by both sorting and degradation, as they increased with decreasing particle size (fine and ultrafine fractions had the most degraded signal and are preferentially transported to the outer shelf) and across the shelf in each of the fractions.

The carbon preference indices for HMW *n*-alkanes and HMW *n*-alkanoic acids have also been widely applied as degradation proxies for plant waxes in marine sediments (for the ESAS, e.g. van Dongen et al., 2008; Fahl and Stein, 1997; Fernandes and Sicre, 2000; Vonk et al., 2010). It measures the ratio of odd-to-even numbers of carbon chain-lengths of HMW lipids and is based on the preference of odd carbon chain-lengths for HMW *n*-alkanes in fresh plant material (even carbon chain-lengths for HMW *n*-alkanoic acids; Eglinton and

569 Hamilton, 1967). With ongoing degradation this preference is lost and the CPI approaches 1
570 (Bray and Evans, 1961).
571 We observed that the HMW *n*-alkane CPI presented a similar pattern as the lignin phenol
572 based degradation indices. However, the HMW *n*-alkanoic acid CPI did not show as much of
573 a degradation trend (HMW *n*-alkane CPI: ~5.7 close to the coast, ~2.2 for the deep stations;
574 HMW *n*-alkanoic acids: ~5.4 close to the coast, ~4.1 for the deep stations; Fig. 6B). Karlsson
575 et al. (2011) measured lipid CPIs in the Buor-Khaya Bay with 10-80 km distance to the coast
576 and obtained similar results to this ~800 km cross-shelf study, with higher values closer to
577 the river delta (Fig. S2 for comparisons with other studies). Their data appears to have a
578 wider spread, though, which might be due to either the narrower dynamic range. Fahl and
579 Stein (1997) also reported a large range of *n*-alkane CPI values (< 0.2- > 5) for Laptev Sea
580 sediments. Fernandes and Sicre (2000) analyzed sediments from the Kara Sea and from the
581 major rivers discharging into this sea, Ob and Yenisey rivers. In the marine environment and
582 the Ob River, they observed HMW *n*-alkane CPI values between 4.8 and 5.3, similar to those
583 found at shallow water depths in this study. For the Yenisey River and mixing zone, they
584 found higher CPI values, pointing to fresher material being transported there. Vonk et al.
585 (2010) recorded HMW *n*-alkane CPI values for sediments along the East Siberian Sea
586 Kolyma paleoriver transect (across the East Siberian Sea) shelf that decreased from > 7.5 to
587 < 4.0 with increasing distance from the river mouth, overall higher than in this study but
588 confirming the general trend to more degraded material on the outer shelf. Tesi et al. (2016)
589 found HMW *n*-alkanoic acid CPI values to decrease with decreasing particle size with no
590 significant trends across the shelf in all but the low-density fraction, which is largely retained
591 close to the shore. The HMW *n*-alkane CPI values in that study, however, showed no
592 systematical differences between different fractions, but an overall decreasing trend with
593 increasing distance from the coast.
594 When undergoing degradation, HMW *n*-alkanoic acids may also lose their functional groups,
595 turning them into HMW *n*-alkanes (Meyers and Ishiwatari, 1993). The slightly decreasing
596 ratio of HMW *n*-alkanoic acids to *n*-alkanes also hints at more degraded material with

increasing water depth, although, due to a rather large variability, this trend is not significant. For the Buor-Khaya Bay surface sediments Karlsson et al. (2011) obtained similar results (0.48-10.7, here 1.1-10.9) with higher values closer to the river delta (Fig. S2 for comparisons with other studies). Along the Kolyma paleoriver transect, Vonk et al. (2010) measured HMW *n*-alkanoic acid to *n*-alkane ratios between 1 and 6 with no clear trend with increasing distance from the river mouth. Tesi et al. (2016) found decreasing values with increasing distance from the coast with no differences between the fractions. Two sediment cores from inner and outer East Siberian Sea recording about one century of sedimentation showed no clear trend in CPI or HMW *n*-alkanoic acid/*n*-alkane towards more degraded TerrOC with increasing sediment depth (Bröder et al., 2016), but displayed a similar difference between inner and outer shelf as seen in this study. This contrasting behavior for cross-shelf and down-core trends may be caused by significantly different timescales for the two processes: about one century in situ/after burial compared to potentially several millennia long lateral transport. Furthermore, the degradation efficiency is likely higher under the oxic conditions prevailing during cross-shelf lateral transport (Keil et al., 2004), than in the anoxic conditions that predominate below a few millimeters of sediments on the ESAS (e.g. Boetius and Damm, 1998). Comparing in situ to transport-related oxygen exposure times on the wide Arctic shelves could potentially resolve the observed discrepancies.

## 4 Concluding remarks and future research directions

Across the Laptev Sea from the Lena River mouth to the deep sea of the Arctic interior a considerable loss of terrigenous organic matter has been observed on both bulk and molecular level. All terrigenous biomarkers display a massive decline with increasing water depth along this high-resolution transect due to hydrodynamic sorting and degradation during transport. Terrigenous organic matter (TerrOC) seems to be also qualitatively more degraded on the outer shelf, slope and rise compared to inner shelf and coastal areas.

These results corroborate and expand previous findings for the East Siberian Arctic Shelf, showing that the shelf seas in this region function as an active reactor for TerrOC. Since the East Siberian Arctic Shelf belongs to the widest and shallowest continental margins on Earth, cross-shelf transport times and thus the time spent in oxic sediments are expected to be comparatively long. This stands in contrast to e.g. the Mackenzie basin, which is thought to act as a geological sink for organic carbon due to its TerrOC burial (Hilton et al., 2015). For narrower Arctic shelves in general, where transport times can be expected to be much shorter, organic matter transfer towards the deeper basins appears to be much more efficient, with high TerrOC concentrations in surface sediments even at greater water depths (e.g. Barrow Canyon, Goni et al., 2013). It can therefore be assumed that the cross-shelf transport time exerts first-order control over the extent of TerrOC degradation. With ongoing global warming, rising permafrost-derived organic carbon input from river-sediment discharge and coastal erosion is expected to reach the marine environment. It is therefore crucial to better constrain cross-shelf transport times in order to determine a TerrOC degradation rate and thereby contribute to quantifying potential carbon-climate feedbacks.

## Acknowledgements

We thank crew and personnel of the IB *ODEN*, the RV *Yakob Smirnitskyi* and the *TB0012*. The SWERUS-C3 and the International Siberian Shelf Study 2008 (ISSS-08) expeditions were supported by the Knut and Alice Wallenberg Foundation, Headquarters of the Far

642 Eastern Branch of the Russian Academy of Sciences, the Swedish Research Council (VR
643 Contract No. 621-2004-4039, 621-2007-4631 and 621-2013-5297), the US National Oceanic
644 and Atmospheric Administration (OAR Climate Program Office, NA08OAR4600758/Siberian
645 Shelf Study), the Russian Foundation of Basic Research RFFI (08-05-13572, 08-05-00191-a,
646 and 07-05-00050a), the Swedish Polar Research Secretariat, the Nordic Council of Ministers
647 and the US National Science Foundation (OPP ARC 0909546). L. Bröder also acknowledges
648 financial support from the Climate Research School of the Bolin Climate Research Centre. T.
649 Tesi also acknowledges EU financial support as a Marie Curie fellow (contract no. PIEF-GA-
650 2011-300259), contribution no. XXXX of ISMAR-CNR Sede di Bologna. J.A. Salvadó also
651 acknowledges EU financial support as a Marie Curie grant (FP7-PEOPLE-2012-IEF; project
652 328049). I. Semiletov thanks the Russian Government for financial support (mega-grant
653 #14.Z50.31.0012). O. Dudarev thanks the Russian Science Foundation (grant No. 15-17-
654 20032).

## References


Aller, R. C. and Blair, N. E.: Carbon remineralization in the Amazon-Guianas tropical mobile mudbelt: A sedimentary incinerator, Continental Shelf Research, 26(17-18), 2241–2259, doi:10.1016/j.csr.2006.07.016, 2006.

Amon, R. M. W., Rinehart, A. J., Duan, S., Louchouarn, P., Prokushkin, A., Guggenberger, G., Bauch, D., Stedmon, C., Raymond, P. A., Holmes, R. M., McClelland, J. W., Peterson, B. J., Walker, S. A. and Zhulidov, A. V.: Dissolved organic matter sources in large Arctic rivers, Geochimica et Cosmochimica Acta, 94, 217–237, doi:10.1016/j.gca.2012.07.015, 2012.

Belicka, L. L., Macdonald, R. W., Yunker, M. B. and Harvey, H. R.: The role of depositional regime on carbon transport and preservation in Arctic Ocean sediments, Marine Chemistry, 86(1-2), 65–88, doi:10.1016/j.marchem.2003.12.006, 2004.

Blair, N. E. and Aller, R. C.: The Fate of Terrestrial Organic Carbon in the Marine Environment, Annual Review of Marine Science, 4(1), 401–423, doi:10.1146/annurev-marine-120709-142717, 2012.

Boetius, A. and Damm, E.: Benthic oxygen uptake, hydrolytic potentials and microbial biomass at the Arctic continental slope, Deep-Sea Research Part I: Oceanographic Research Papers, 45(2-3), 239–275, doi:10.1016/S0967-0637(97)00052-6, 1998.

Boetius, A., Albrecht, S., Bakker, K., Bienhold, C., Felden, J., Fernández-Méndez, M., Hendricks, S., Katlein, C., Lalande, C., Krumpen, T., Nicolaus, M., Peeken, I., Rabe, B., Rogacheva, A., Rybakova, E., Somavilla, R. and Wenzhöfer, F.: Export of algal biomass from the melting Arctic sea ice., Science (New York, N.Y.), 339(6126), 1430–2, doi:10.1126/science.1231346, 2013.

Bray, E. . and Evans, E. .: Distribution of n-paraffins as a clue to recognition of source beds, Geochimica et Cosmochimica Acta, 22(1), 2–15, doi:10.1016/0016-7037(61)90069-2, 1961.

Brunauer, S., Emmett, P. H. and Teller, E.: Adsorption of Gases in Multimolecular Layers, Journal of the American Chemical Society, 60(2), 309–319, doi:citeulike-article-id:4074706\rdoi: 10.1021/ja01269a023, 1938.

Bröder, L., Tesi, T., Andersson, A., Eglinton, T. I., Semiletov, I. P., Dudarev, O. V., Roos, P. and Gustafsson, Ö.: Historical records of organic matter supply and degradation status in the East Siberian Sea, Organic Geochemistry, 91, 16–30, doi:10.1016/j.orggeochem.2015.10.008, 2016.

Charkin, A. N., Dudarev, O. V., Semiletov, I. P., Kruhmalev, A. V., Vonk, J. E., Sánchez-García, L., Karlsson, E., Gustafsson, O., Gustafsson, Ö. and Gustafsson, O.: Seasonal and interannual variability of sedimentation and organic matter distribution in the Buor-Khaya Gulf: The primary recipient of input from Lena River and coastal erosion in the southeast Laptev Sea, Biogeosciences, 8(9), 2581–2594, doi:10.5194/bg-8-2581-2011, 2011.

Dethleff, D.: Entrainment and export of Laptev Sea ice sediments, Siberian Arctic, Journal of Geophysical Research C: Oceans, 110(7), 1–17, doi:10.1029/2004JC002740, 2005.

Dethleff, D.: Dense water formation in the Laptev Sea flaw lead, Journal of Geophysical Research: Oceans, 115(12), 1–16, doi:10.1029/2009JC006080, 2010.

Dickens, A. F., Gudeman, J. A., Gélinas, Y., Baldock, J. A., Tinner, W., Hu, F. S. and Hedges, J. I.: Sources and distribution of CuO-derived benzene carboxylic acids in soils and sediments, Organic Geochemistry, 38(8), 1256–1276, doi:10.1016/j.orggeochem.2007.04.004, 2007.

Dmitrenko, I. A., Kirillov, S. A. and Bruno Tremblay, L.: The long-term and interannual variability of summer fresh water storage over the eastern Siberian shelf: Implication for climatic change, Journal of Geophysical Research: Oceans, 113(3), 1–14, doi:10.1029/2007JC004304, 2008.

Eglinton, G. and Hamilton, R. J.: Leaf epicuticular waxes., Science (New York, N.Y.), 156(780), 1322–1335, doi:10.1126/science.156.3780.1322, 1967.

Eicken, H., Reimnitz, E., Alexandrov, V., Martin, T., Kassens, H. and Viehoff, T.: Sea-ice processes in the Laptev Sea and their importance for sediment export, Continental Shelf Research, 17(2), 205–233, doi:10.1016/S0278-4343(96)00024-6, 1997.

Ertel, J. R. and Hedges, J. I.: The lignin component of humic substances: Distribution among soil and sedimentary humic, fulvic, and base-insoluble fractions, Geochimica et Cosmochimica Acta, 48(10), 2065–2074, doi:10.1016/0016-7037(84)90387-9, 1984.

Fahl, K. and Stein, R.: Modern organic carbon deposition in the Laptev Sea and the adjacent continental slope:

Surface water productivity vs. terrigenous input, Organic Geochemistry, 26(5-6), 379–390, doi:10.1016/S0146-6380(97)00007-7, 1997.

Feng, X., Vonk, J. E., van Dongen, B. E., Gustafsson, Ö., Semiletov, I. P., Dudarev, O. V, Wang, Z., Montluçon, D. B., Wacker, L. and Eglinton, T. I.: Differential mobilization of terrestrial carbon pools in Eurasian Arctic river basins., Proceedings of the National Academy of Sciences of the United States of America, 110(35), 14168–73, doi:10.1073/pnas.1307031110, 2013.

Feng, X., Gustafsson, Ö., Holmes, R. M., Vonk, J. E., van Dongen, B. E., Semiletov, I. P., Dudarev, O. V., Yunker, M. B., Macdonald, R. W., Montluçon, D. B. and Eglinton, T. I.: Multi-molecular tracers of terrestrial carbon transfer across the pan-Arctic – Part 1: Comparison of hydrolysable components with plant wax lipids and lignin phenols, Biogeosciences Discussions, 12(6), 4721–4767, doi:10.5194/bgd-12-4721-2015, 2015.

Fernandes, M. B. and Sicre, M. A.: The importance of terrestrial organic carbon inputs on Kara Sea shelves as revealed by n-alkanes, OC and d13C values, in Organic Geochemistry, vol. 31, pp. 363–374., 2000.

Fry, B. and Sherr, E. B.: d13C Measurements as indicators of carbon flow in marine and freshwater ecosystems, Contributions in Marine Science, 27, 13–49, 1984.

Goni, M. A., O'Connor, A. E., Kuzyk, Z. Z., Yunker, M. B., Gobeil, C. and Macdonald, R. W.: Distribution and sources of organic matter in surface marine sediments across the North American Arctic margin, Journal of Geophysical Research-Oceans, 118(9), 4017–4035, doi:10.1002/jgrc.20286, 2013.

Goñi, M. A. and Hedges, J. I.: Sources and reactivities of marine-derived organic matter in coastal sediments as determined by alkaline CuO oxidation, Geochimica et Cosmochimica Acta, 59(14), 2965–2981, doi:10.1016/0016-7037(95)00188-3, 1995.

Goñi, M. A. and Montgomery, S.: Alkaline CuO oxidation with a microwave digestion system: Lignin analyses of geochemical samples, Analytical Chemistry, 72(14), 3116–3121, doi:10.1021/ac991316w, 2000.

Goñi, M. A., Ruttenberg, K. C. and Eglinton, T. I.: A reassessment of the sources and importance of land-derived organic matter in surface sediments from the Gulf of Mexico, Geochimica et Cosmochimica Acta, 62(18), 3055–3075, doi:10.1016/S0016-7037(98)00217-8, 1998.

Goñi, M. A., Yunker, M. B., MacDonald, R. W. and Eglinton, T. I.: Distribution and sources of organic biomarkers in arctic sediments from the Mackenzie River and Beaufort Shelf, Marine Chemistry, 71(1-2), 23–51, doi:10.1016/S0304-4203(00)00037-2, 2000.

Gordeev, V. V.: Fluvial sediment flux to the Arctic Ocean, Geomorphology, 80(1-2), 94–104, doi:10.1016/j.geomorph.2005.09.008, 2006.

Gordon, E. S. and Goñi, M. A.: Controls on the distribution and accumulation of terrigenous organic matter in sediments from the Mississippi and Atchafalaya river margin, Marine Chemistry, 92(1-4 SPEC. ISS.), 331–352, doi:10.1016/j.marchem.2004.06.035, 2004.

Guay, C. K. H., Falkner, K. K., Muench, R. D., Mensch, M., Frank, M. and Bayer, R.: Wind-driven transport for Eurasian Arctic rover discharge, Journal of Geophysical Research, 106(C6), 11469–11480, 2001.

Gustafsson, Ö., Van Dongen, B. E., Vonk, J. E., Dudarev, O. V. and Semiletov, I. P.: Widespread release of old carbon across the Siberian Arctic echoed by its large rivers, Biogeosciences, 8(6), 1737–1743, doi:10.5194/bg-8-1737-2011, 2011.

Günther, F., Overduin, P. P., Sandakov, A. V., Grosse, G. and Grigoriev, M. N.: Short- and long-term thermo-erosion of ice-rich permafrost coasts in the Laptev Sea region, Biogeosciences, 10(6), 4297–4318, doi:10.5194/bg-10-4297-2013, 2013.

Hedges, J. I. and Mann, D. C.: The characterization of plant tissues by their lignin oxidation products, Geochimica et Cosmochimica Acta, 43(11), 1803–1807, doi:10.1016/0016-7037(79)90028-0, 1979a.

Hedges, J. I. and Mann, D. C.: The lignin geochemistry of marine sediments from the southern Washington coast, Geochimica et Cosmochimica Acta, 43(11), 1809–1818, doi:10.1016/0016-7037(79)90029-2, 1979b.

Hedges, J. I. and Parker, P. L.: Land-derived organic matter in surface sediments from the Gulf of Mexico, Geochimica et Cosmochimica Acta, 40, 1019–1029, 1976.

Hedges, J. I., Blanchette, R. A., Weliky, K. and Devol, A. H.: Effects of fungal degradation on the CuO oxidation products of lignin: A controlled laboratory study, Geochimica et Cosmochimica Acta, 52(11), 2717–2726, doi:10.1016/0016-7037(88)90040-3, 1988.

754 Hilton, R. G., Galy, V., Gaillardet, J., Dellinger, M., Bryant, C., O'Regan, M., Gröcke, D. R., Coxall, H., Bouchez, J.
755 and Calmels, D.: Erosion of organic carbon in the Arctic as a geological carbon dioxide sink, Nature, 524(7563),
756 84–87, doi:10.1038/nature14653, 2015.

757 Holmes, R. M., McClelland, J. W., Peterson, B. J., Shiklomanov, I. A., Shiklomanov, A. I., Zhulidov, A. V,
758 Gordeev, V. V and Bobrovitskaya, N. N.: A circumpolar perspective on fluvial sediment flux to the Arctic ocean,
759 Global Biogeochemical Cycles, 16(4), 14–45, doi:10.1029/2001GB001849, 2002.

760 Holmes, R. M., McClelland, J. W., Peterson, B. J., Tank, S. E., Bulygina, E., Eglinton, T. I., Gordeev, V. V.,
761 Gurtovaya, T. Y., Raymond, P. a., Repeta, D. J., Staples, R., Striegl, R. G., Zhulidov, A. V. and Zimov, S. a.:
762 Seasonal and Annual Fluxes of Nutrients and Organic Matter from Large Rivers to the Arctic Ocean and
763 Surrounding Seas, Estuaries and Coasts, 35(2), 369–382, doi:10.1007/s12237-011-9386-6, 2012.

764 Hugelius, G., Strauss, J., Zubrzycki, S., Harden, J. W., Schuur, E. A. G., Ping, C. L., Schirrmeister, L., Grosse, G.,
765 Michaelson, G. J., Koven, C. D., O'Donnell, J. A., Elberling, B., Mishra, U., Camill, P., Yu, Z., Palmtag, J. and
766 Kuhry, P.: Improved estimates show large circumpolar stocks of permafrost carbon while quantifying substantial
767 uncertainty ranges and identifying remaining data gaps, Biogeosciences Discussions, 11(3), 4771–4822,
768 doi:10.5194/bgd-11-4771-2014, 2014.

769 Ivanov, V. V. and Golovin, P. N.: Observations and modeling of dense water cascading from the northwestern
770 Laptev Sea shelf, Journal of Geophysical Research: Oceans, 112(9), 1–15, doi:10.1029/2006JC003882, 2007.

771 Jakobsson, M., Grantz, A., Kristoffersen, Y. and Macnab, R.: Physiography and Bathymetry of the Arctic Ocean,
772 in The Organic Carbon Cycle in the Arctic Ocean, edited by R. Stein and R. W. Macdonald, pp. 1–5., 2004.

773 Karlsson, E. S., Charkin, A., Dudarev, O., Semiletov, I., Vonk, J. E., Sánchez-García, L. and Andersson, A.:
774 Carbon isotopes and lipid biomarker investigation of sources, transport and degradation of terrestrial organic
775 matter in the Buor-Khaya Bay, SE Laptev Sea, Biogeosciences, 8(7), 1865–1879, doi:10.5194/bg-8-1865-2011,
776 2011.

777 Karlsson, E. S., Brüchert, V., Tesi, T., Charkin, a, Dudarev, O., Semiletov, I. and Gustafsson, Ö.: Contrasting
778 regimes for organic matter degradation in the East Siberian Sea and the Laptev Sea assessed through microbial
779 incubations and molecular markers, Marine Chemistry, 170, 11–22, doi:10.1016/j.marchem.2014.12.005, 2014.

780 Keil, R. G., Tsamakis, E., Fuh, C. B., Giddings, J. C. and Hedges, J. I.: Mineralogical and textural controls on the
781 organic composition of coastal marine sediments: Hydrodynamic separation using SPLITT-fractionation,
782 Geochimica et Cosmochimica Acta, 58(2), 879–893, doi:10.1016/0016-7037(94)90512-6, 1994.

783 Keil, R. G., Mayer, L. M., Quay, P. D., Richey, J. E. and Hedges, J. I.: Loss of organic matter from riverine
784 particles in deltas, Geochimica et Cosmochimica Acta, 61(7), 1507–1511, doi:10.1016/S0016-7037(97)00044-6,
785 1997a.

786 Keil, R. G., Tsamakis, E. and Wolf, N.: Relationships between organic carbon preservation and mineral surface
787 area in Amazon fan sediments (Holes 932A and 942A), Proceedings of the Ocean Drilling Program, 155, 531–
788 538 [online] Available from: http://cat.inist.fr/?aModele=afficheN&cpsidt=2169716, 1997b.

789 Keil, R. G., Dickens, A. F., Arnarson, T., Nunn, B. L. and Devol, A. H.: What is the oxygen exposure time of
790 laterally transported organic matter along the Washington margin?, Marine Chemistry, 92(1-4 SPEC. ISS.), 157–
791 165, doi:10.1016/j.marchem.2004.06.024, 2004.

792 Macdonald, R. W., Naidu, A. S., Yunker, M. B. and Gobeil, C.: The Beaufort Sea: distribution, sources, fluxes and
793 burial of organic carbon, in The Organic Carbon Cycle in the Arctic Ocean, edited by R. Stein and R. W.
794 Macdonald, pp. 177–192., 2004.

795 Magen, C., Chaillou, G., Crowe, S. a., Mucci, A., Sundby, B., Gao, A., Makabe, R. and Sasaki, H.: Origin and fate
796 of particulate organic matter in the southern Beaufort Sea - Amundsen Gulf region, Canadian Arctic, Estuarine,
797 Coastal and Shelf Science, 86(1), 31–41, doi:10.1016/j.ecss.2009.09.009, 2010.

798 Mammone, K. A.: Sediment provenance and transport on the Siberian Arctic shelf, Oregon State University.,
799 1998.

800 Mayer, L. M.: Surface area control of organic carbon accumulation in continental shelf sediments, Geochimica et
801 Cosmochimica Acta, 58(4), 1271–1284, doi:10.1016/0016-7037(94)90381-6, 1994.

802 Mayer, L., Benninger, L., Bock, M., DeMaster, D., Roberts, Q. and Martens, C.: Mineral associations and
803 nutritional quality of organic matter in shelf and upper slope sediments off Cape Hatteras, USA: A case of
804 unusually high loadings, Deep-Sea Research Part II: Topical Studies in Oceanography, 49(20), 4587–4597,
805 doi:10.1016/S0967-0645(02)00130-3, 2002.

McClelland, J. W., Holmes, R. M., Peterson, B. J., Amon, R., Brabets, T., Cooper, L., Gibson, J., Gordeev, V. V., Guay, C., Milburn, D., Staples, R., Raymond, P. A., Shiklomanov, I., Stiegl, R., Zhulidov, A., Gurtovaya, T. and Zimov, S.: Development of a Pan-Arctic Database for River Chemistry From Corals to Canyons : The Great Barrier Reef Margin, Program, 89(24), 217–218, doi:10.1029/2006JG000353., 2008.

Mercone, D., Thomson, J., Abu-Zied, R. H., Croudace, I. W. and Rohling, E. J.: High-resolution geochemical and micropalaeontological profiling of the most recent eastern Mediterranean sapropel, Marine Geology, 177(1-2), 25–44, doi:10.1016/S0025-3227(01)00122-0, 2001.

Meyers, P. A. and Ishiwatari, R.: Lacustrine organic geochemistry-an overview of indicators of organic matter sources and diagenesis in lake sediments, Organic Geochemistry, 20(7), 867–900, doi:10.1016/0146-6380(93)90100-P, 1993.

Naidu, A. S., Cooper, L. W., Finney, B. P., Macdonald, R. W., Alexander, C. and Semiletov, I. P.: Organic carbon isotope ratio (d13C) of Arctic Amerasian Continental shelf sediments, International Journal of Earth Sciences, 89(3), 522–532, doi:10.1007/s005310000121, 2000.

Nieuwenhuize, J., Maas, Y. E. . and Middelburg, J. J.: Rapid analysis of organic carbon and nitrogen in particulate materials, Marine Chemistry, 45(3), 217–224, doi:10.1016/0304-4203(94)90005-1, 1994.

Opsahl, S. and Benner, R.: Early diagenesis of vascular plant tissues : Lignin and cutin decomposition and biogeochemical implications, Geochimica et Cosmochimica Acta, 59(23), 4889–4904, 1995.

Panova, E., Tesi, T., Pearce, C., Salvadó, J. A., Karlsson, E. S., Kruså, M., Semiletov, I. P. and Gustafsson, Ö.: Geochemical compositional differences of the supramicron plankton-dominated fraction in two regimes of the Marginal Ice Zone (MIZ) of the outer East Siberian Arctic Shelf, in AGU Fall Meeting, p. Conference Abstract C43A–0797., 2015.

Pearson, A., Mcnichol, A. P., Schneider, R. J., von Reden, K. F. and Zheng, Y.: Microscale AMS 14C measurement at NOSAMS, Radiocarbon, 40(1), 61–75, 1998.

Prahl, F. G., Ertel, J. R., Goni, M. A., Sparrow, M. A. and Eversmeyer, B.: Terrestrial organic carbon contributions to sediments on the Washington margin, Geochimica et Cosmochimica Acta, 58(14), 3035–3048, doi:10.1016/0016-7037(94)90177-5, 1994.

Rachold, V. and Hubberten, H. W.: Carbon isotope composition of particulate organic material in east Siberian rivers, Land-Ocean Systems in the Siberian Arctic: Dynamics and History, 223–238, 1998.

Rachold, V., Grigoriev, M. N., Are, F. E., Solomon, S., Reimnitz, E., Kassens, H. and Antonow, M.: Coastal erosion vs riverine sediment discharge in the Arctic Shelf seas, International Journal of Earth Sciences, 89(3), 450–459, doi:10.1007/s005310000113, 2000.

Rachold, V., Eicken, H., Gordeev, V. V, Grigoriev, M. N., Hubberten, H.-W., Lisitzin, A. P., Shevchenko, V. P. and Schirrmeister, L.: Modern Terrigenous Organic Carbon Input to the \textsc{A}rctic \textsc{O}cean, The Organic Carbon Cycle in the Arctic Ocean, 33–55, 2004.

Sakshaug, E.: Primary and secondary production in the Arctic Seas, in The Organic Carbon Cycle in the Arctic Ocean, edited by R. Stein and R. W. Macdonald, pp. 57–81., 2004.

Salvadó, J. A., Tesi, T., Andersson, A., Ingri, J., Dudarev, O. V., Semiletov, I. P. and Gustafsson, Ö.: Organic carbon remobilized from thawing permafrost is resequestered by reactive iron on the Eurasian Arctic Shelf, Geophysical Research Letters, 42(19), 8122–8130, doi:10.1002/2015GL066058, 2015.

Sánchez-García, L., Alling, V., Pugach, S., Vonk, J., Van Dongen, B., Humborg, C., Dudarev, O., Semiletov, I. and Gustafsson, Ö.: Inventories and behavior of particulate organic carbon in the Laptev and East Siberian seas, Global Biogeochemical Cycles, 25(2), 1–13, doi:10.1029/2010GB003862, 2011.

Schubert, C. J. and Calvert, S. E.: Nitrogen and carbon isotopic composition of marine and terrestrial organic matter in Arctic Ocean sediments:, Deep Sea Research Part I: Oceanographic Research Papers, 48(3), 789–810, doi:10.1016/S0967-0637(00)00069-8, 2001.

Semiletov, I.P., Destruction of the coastal permafrost ground as an important factor in biogeochemistry of the Arctic Shelf waters, Trans. (Doklady) Russian Acad. Sci., 368, 679-682, 1999 (translated into English).

Semiletov, I. and Gustafsson, Ö.: East Siberian Shelf Study Alleviates Scarcity of Observations, Eos, Transactions American Geophysical Union, 90(17), 145, doi:10.1029/2009EO170001, 2009.

Semiletov, I., Dudarev, O., Luchin, V., Charkin, A., Shin, K. H. and Tanaka, N.: The East Siberian Sea as a

856 transition zone between Pacific-derived waters and Arctic shelf waters, Geophysical Research Letters, 32(10), 1–
857 5, doi:10.1029/2005GL022490, 2005.

858 Semiletov, I. P., Pipko, I. I., Shakhova, N. E., Dudarev, O. V., Pugach, S. P., Charkin, A. N., Mcroy, C. P.,
859 Kosmach, D. and Gustafsson, Ö.: Carbon transport by the Lena River from its headwaters to the Arctic Ocean,
860 with emphasis on fluvial input of terrestrial particulate organic carbon vs. carbon transport by coastal erosion,
861 Biogeosciences, 8(9), 2407–2426, doi:10.5194/bg-8-2407-2011, 2011.

862 Semiletov, I. P., Shakhova, N. E., Sergienko, V. I., Pipko, I. I. and Dudarev, O. V: On carbon transport and fate in
863 the East Siberian Arctic land–shelf–atmosphere system, Environmental Research Letters, 7(1), 015201,
864 doi:10.1088/1748-9326/7/1/015201, 2012.

865 Semiletov, I. P., Shakhova, N. E., Pipko, I. I., Pugach, S. P., Charkin, A. N., Dudarev, O. V., Kosmach, D. A. and
866 Nishino, S.: Space-time dynamics of carbon and environmental parameters related to carbon dioxide emissions in
867 the Buor-Khaya Bay and adjacent part of the Laptev Sea, Biogeosciences, 10(9), 5977–5996, doi:10.5194/bg-10-
868 5977-2013, 2013.

869 Semiletov, I., Pipko, I., Gustafsson, Ö., Anderson, L. G., Sergienko, V., Pugach, S., Dudarev, O., Charkin, A.,
870 Gukov, A., Bröder, L., Andersson, A., Spivak, E. and Shakhova, N.: Acidification of East Siberian Arctic Shelf
871 waters through addition of freshwater and terrestrial carbon, Nature Geoscience, (April), doi:10.1038/NEGO2695,
872 2016.

873 Shakhova, N., Semiletov, I., Sergienko, V., Lobkovsky, L., Yusupov, V., Salyuk, A., Salomatin, A., Chernykh, D.,
874 Kosmach, D., Panteleev, G., Nicolsky, D., Samarkin, V., Joye, S., Charkin, A., Dudarev, O., Meluzov, A. and
875 Gustafsson, O.: The East Siberian Arctic Shelf: towards further assessment of permafrost-related methane fluxes
876 and role of sea ice., Philosophical transactions. Series A, Mathematical, physical, and engineering sciences,
877 373(2052), 20140451–, doi:10.1098/rsta.2014.0451, 2015.

878 Stein, R. and Fahl, K.: Holocene accumulation of organic carbon at the Laptev Sea continental margin (Arctic
879 Ocean): sources, pathways, and sinks, Geo-Marine Letters, 20(1), 27–36, doi:10.1007/s003670000028, 2000.

880 Stein, R. and Fahl, K.: The Laptev Sea: Distribution, Sources, Variability and Burial of Organic Carbon, in The
881 Organic Carbon Cycle in the Arctic Ocean, edited by R. Stein and R. W. Macdonald, pp. 213–236., 2004.

882 Stein, R. and Macdonald, R. W., Eds.: The organic carbon cycle in the Arctic Ocean, Springer Verlag., 2004.

883 Stuvier, M. and Polach, H. A.: Reporting of 14C Data, Radiocarbon, 19(3), 355–363,
884 doi:10.1016/j.forsciint.2010.11.013, 1977.

885 Syvitski, J. P. M.: Sediment discharge variability in Arctic rivers: Implications for a warmer future, Polar Research,
886 21(2), 323–330, doi:10.1111/j.1751-8369.2002.tb00087.x, 2002.

887 Tarnocai, C., Canadell, J. G., Schuur, E. A. G., Kuhry, P., Mazhitova, G. and Zimov, S.: Soil organic carbon pools
888 in the northern circumpolar permafrost region, Global Biogeochemical Cycles, 23(2), 1–11,
889 doi:10.1029/2008GB003327, 2009.

890 Tesi, T., Semiletov, I., Hugelius, G., Dudarev, O., Kuhry, P. and Gustafsson, Ö.: Composition and fate of
891 terrigenous organic matter along the Arctic land-ocean continuum in East Siberia: Insights from biomarkers and
892 carbon isotopes, Geochimica et Cosmochimica Acta, 133, 235–256, doi:10.1016/j.gca.2014.02.045, 2014.

893 Tesi, T., Semiletov, I., Dudarev, O., Andersson, A. and Gustafsson, Ö.: Matrix association effects on
894 hydrodynamic sorting and degradation of terrestrial organic matter during cross-shelf transport in the Laptev and
895 East Siberian shelf seas, Journal of Geophysical Research: Biogeosciences, 121(3), 731–752,
896 doi:10.1002/2015JG003067, 2016.

897 van Dongen, B. E., Semiletov, I., Weijers, J. W. H. and Gustafsson, Ö.: Contrasting lipid biomarker composition of
898 terrestial organic matter exported from across the Eurasian Arctic by the five great Russian Arctic rivers, Global
899 Biogeochemical Cycles, 22(1), 1–14, doi:10.1029/2007GB002974, 2008a.

900 van Dongen, B. E., Zencak, Z. and Gustafsson, Ö.: Differential transport and degradation of bulk organic carbon
901 and specific terrestrial biomarkers in the surface waters of a sub-arctic brackish bay mixing zone, Marine
902 Chemistry, 112(3-4), 203–214, doi:10.1016/j.marchem.2008.08.002, 2008b.

903 Vonk, J. E. and Gustafsson, Ö.: Permafrost-carbon complexities, Nature Geoscience, 6(9), 675–676,
904 doi:10.1038/ngeo1937, 2013.

905 Vonk, J. E., Sánchez-García, L., Semiletov, I., Dudarev, O., Eglinton, T., Andersson, A. and Gustafsson, O.:

Molecular and radiocarbon constraints on sources and degradation of terrestrial organic carbon along the Kolyma paleoriver transect, East Siberian Sea, Biogeosciences, 7(10), 3153–3166, doi:10.5194/bg-7-3153-2010, 2010.

Vonk, J. E., Sánchez-García, L., van Dongen, B. E., Alling, V., Kosmach, D., Charkin, A., Semiletov, I. P., Dudarev, O. V., Shakhova, N., Roos, P., Eglinton, T. I., Andersson, A. and Gustafsson, Ö.: Activation of old carbon by erosion of coastal and subsea permafrost in Arctic Siberia, Nature, 489(7414), 137–140, doi:10.1038/nature11392, 2012.

Vonk, J. E., Semiletov, I. P., Dudarev, O. V., Eglinton, T. I., Andersson, A., Shakhova, N., Charkin, A., Heim, B. and Gustafsson, Ö.: Preferential burial of permafrost-derived organic carbon in Siberian-Arctic shelf waters, Journal of Geophysical Research: Oceans, 119, 8410–8421, doi:10.1002/2014JC010261.Received, 2014.

Wegner, C., Hölemann, J. A., Dmitrenko, I., Kirillov, S. and Kassens, H.: Seasonal variations in Arctic sediment dynamics - Evidence from 1-year records in the Laptev Sea (Siberian Arctic), Global and Planetary Change, 48(1-3 SPEC. ISS.), 126–140, doi:10.1016/j.gloplacha.2004.12.009, 2005.

Wegner, C., Bauch, D., Hölemann, J. A., Janout, M. A., Heim, B., Novikhin, A., Kassens, H. and Timokhov, L.: Interannual variability of surface and bottom sediment transport on the Laptev Sea shelf during summer, Biogeosciences, 10(2), 1117–1129, doi:10.5194/bg-10-1117-2013, 2013.

Weingartner, T. J., Danielson, S., Sasaki, Y., Pavlov, V. and Kulakov, M.: The Siberian Coastal Current: A wind- and buoyancy-forced Arctic coastal current, Journal of Geophysical Research, 104(C12), 29697, doi:10.1029/1999JC900161, 1999.

Wiesenberg, G. L. B., Schwark, L. and Schmidt, M. W. I.: Improved automated extraction and separation procedure for soil lipid analyses, European Journal of Soil Science, 55(2), 349–356, doi:10.1111/j.1351-0754.2004.00601.x, 2004.

Winterfeld, M., Goñi, M. A., Just, J., Hefter, J. and Mollenhauer, G.: Characterization of particulate organic matter in the Lena River Delta and adjacent nearshore zone, NE Siberia - Part 2: Lignin-derived phenol compositions, Biogeosciences, 12, 2261–2283, doi:10.5194/bgd-11-14359-2014, 2015a.

Winterfeld, M., Laepple, T. and Mollenhauer, G.: Characterization of particulate organic matter in the Lena River delta and adjacent nearshore zone, NE Siberia - Part I: Radiocarbon inventories, Biogeosciences, 12(12), 3769–3788, doi:10.5194/bg-12-3769-2015, 2015b.

Yunker, M. B., Macdonald, R. W., Cretney, W. J., Fowler, B. R., Mclaughlin, F. A. and Bay, R. R. B.: Alkane, terpene, and polycyclic aromatic hydrocarbon geochemistry of the Mackenzie River and Mackenzie shelf." Riverine contributions to Beaufort Sea coastal sediment, , 57, 3041–3061, 1993.

Yunker, M. B., Macdonald, R. W., Veltkamp, D. J. and Cretney, W. J.: Terrestrial and marine biomarkers in a seasonally ice-covered Arctic estuary — integration of multivariate and biomarker approaches, Marine Chemistry, 49(1), 1–50, doi:http://dx.doi.org/10.1016/0304-4203(94)00057-K, 1995.

Yunker, M. B., Belicka, L. L., Harvey, H. R. and Macdonald, R. W.: Tracing the inputs and fate of marine and terrigenous organic matter in Arctic Ocean sediments: A multivariate analysis of lipid biomarkers, Deep-Sea Research Part II: Topical Studies in Oceanography, 52(24-26), 3478–3508, doi:10.1016/j.dsr2.2005.09.008, 2005.

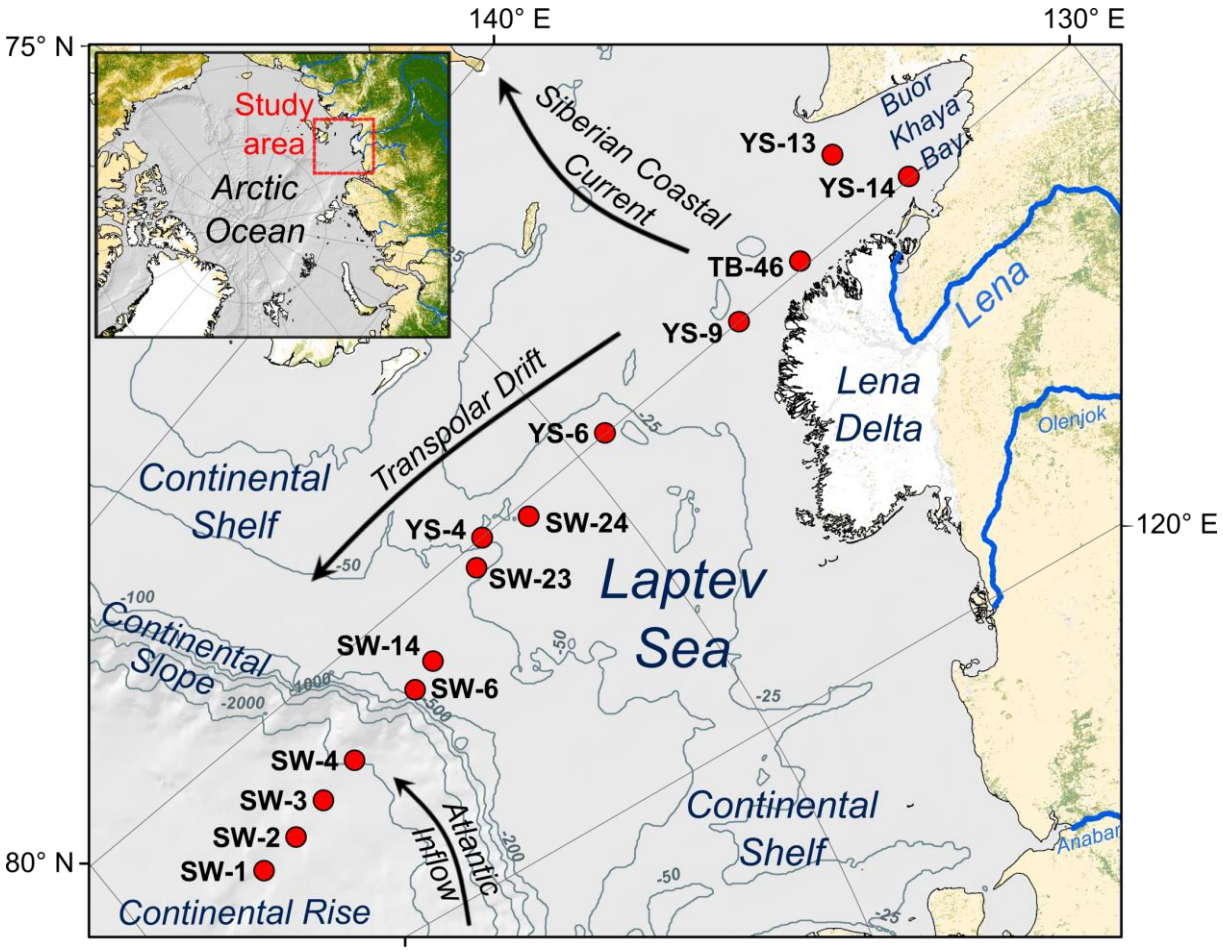


Figure 1: Map of the study area in the Laptev Sea. Red filled circles mark the sediment sampling sites. The transect reaches from the Lena River mouth and the Buor-Khaya Bay (water depths ~10 m) across the Laptev Sea Shelf (mean depth ~50 m) to the slope/shelf break and rise (water depths ~3000 m). Arrows show the directions of the prevailing ocean currents.

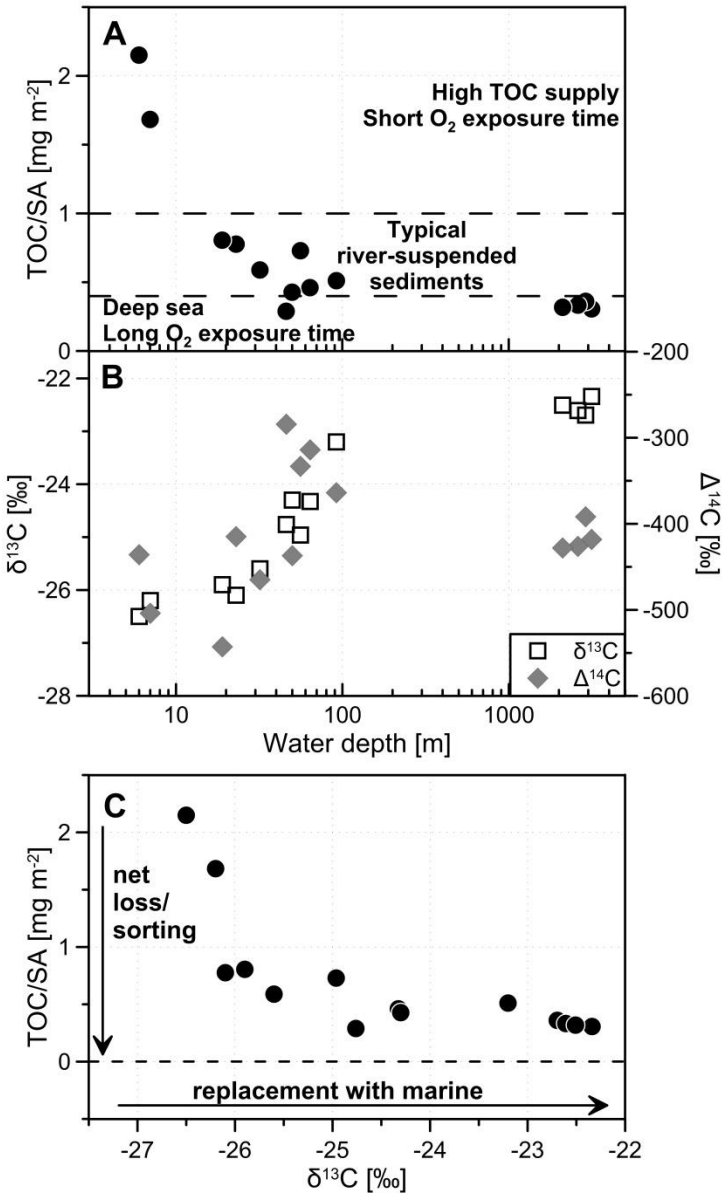


Figure 2: (A) The ratio of total organic carbon (TOC) to mineral surface area (SA). Typical values for deep sea, river-suspended sediments and high TOC supply are taken from Blair and Aller (2012). (B) The stable carbon isotopic signal ($\delta^{13}C$, open boxes) and the radiocarbon isotopic signal ($\Delta^{14}C$, filled diamonds). (C) The relationship between TOC/SA and $\delta^{13}C$ can help to disentangle two processes occurring simultaneously during cross-shelf transport: The net loss (i.e. degradation) or sorting (i.e. hydraulically retaining) of TerrOC leads to a shift towards lower TOC/SA ratios, whereas the replacement/dilution with marine OC shifts the isotopic signature towards higher values.

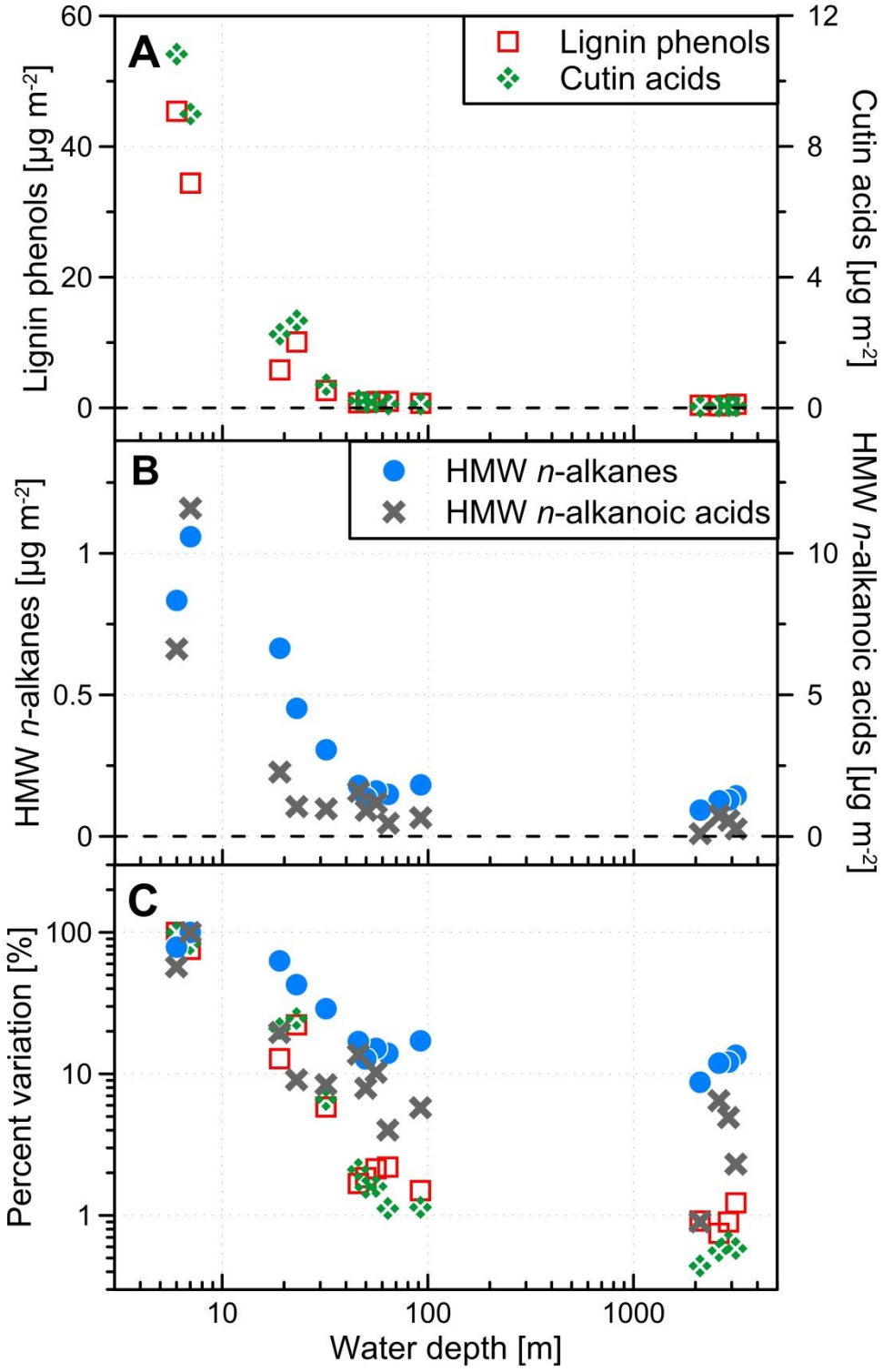


Figure 3: Terrigenous biomarker loadings across the shelf: (A) lignin phenols and cutin acids, (B) HMW *n*-alkanes and HMW *n*-alkanoic acids. (C) Comparison between the different biomarkers along the transect: lignin phenols, cutin acids, HMW *n*-alkanoic acids and *n*-alkanes where each is normalized to respective highest value (corresponding to 100 %).

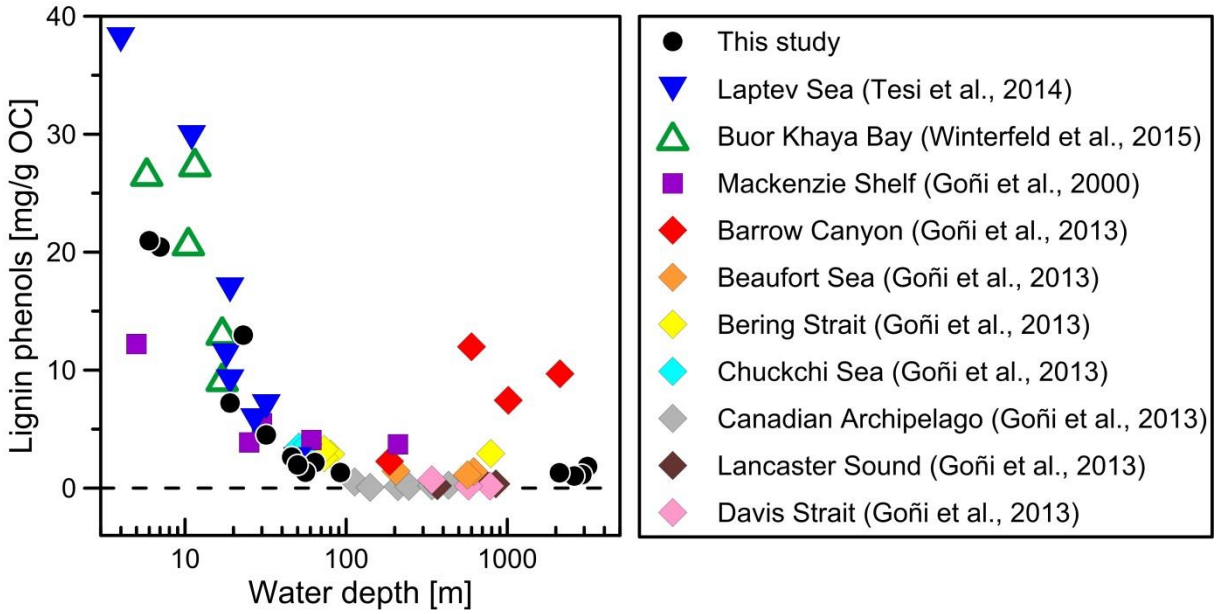


Figure 4: A comparison of lignin phenol data from this project to values from published studies around the Arctic Ocean. Similar decreasing trends with increasing water depth are observed for all systems but Barrow Canyon, where elevated lignin phenols concentrations are found even at depth of > 1000 m.

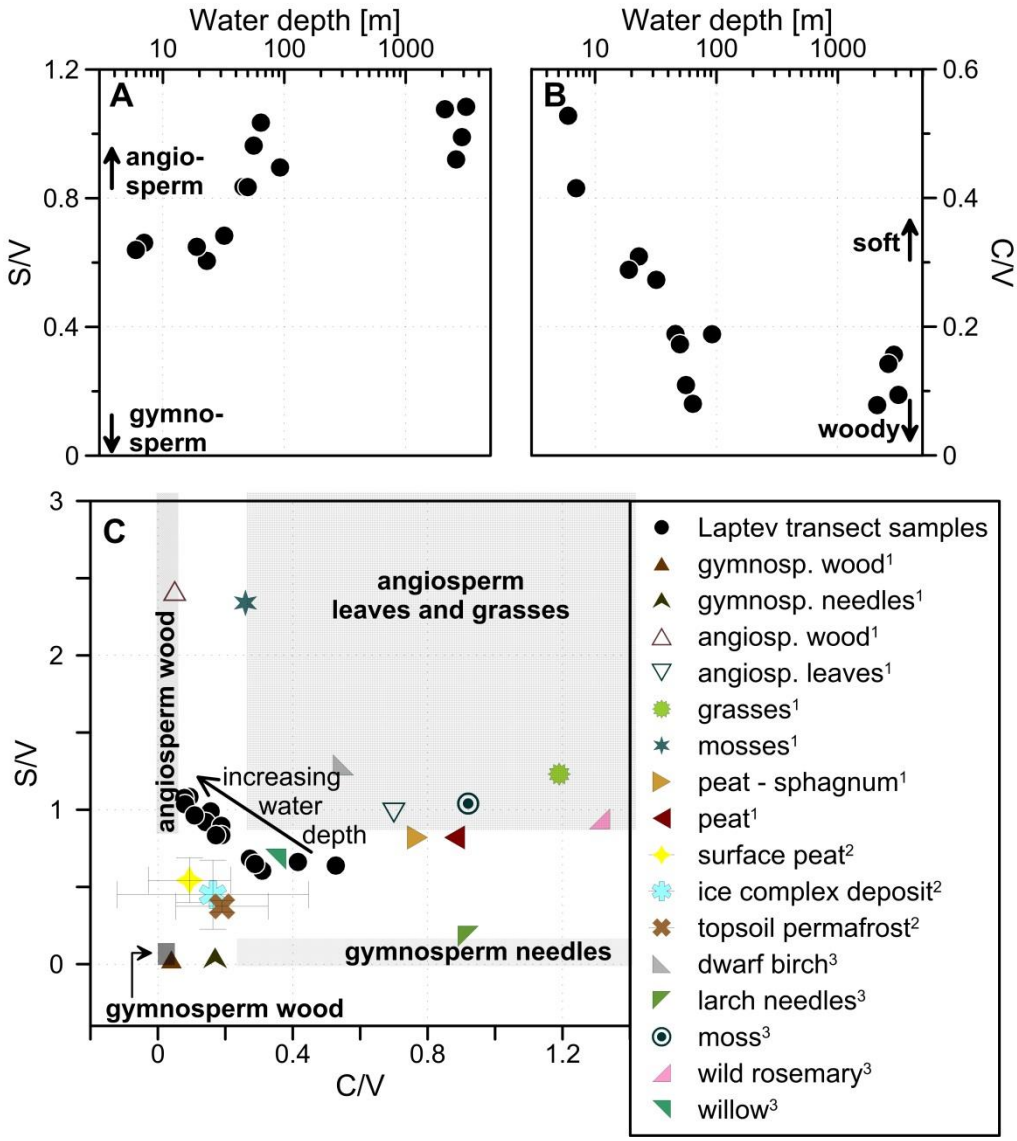


Figure 5: The lignin phenol composition carries source information: (A) an increasing ratio of syringyl to vanillyl phenols (S/V) suggests relatively more angiosperm material. (B) A decreasing ratio of cinnamyl to vanillyl phenols (C/V) implies an increasing relative contribution of woody material compared to soft tissues. (C) Comparison of S/V and C/V with the end-members for different Arctic plants as compiled from different studies by Amon et al. (2012, and citations therein, here marked with [1]); ice-complex deposit and topsoil permafrost as determined by Tesi et al. (2014, here marked with [2]) and more plant species measured by Winterfeld et al. (2015a, here marked with [3]). The boxes indicate typical ranges of S/V and C/V for different vascular plant tissues in different locations (e.g. Goñi et al., 2000).

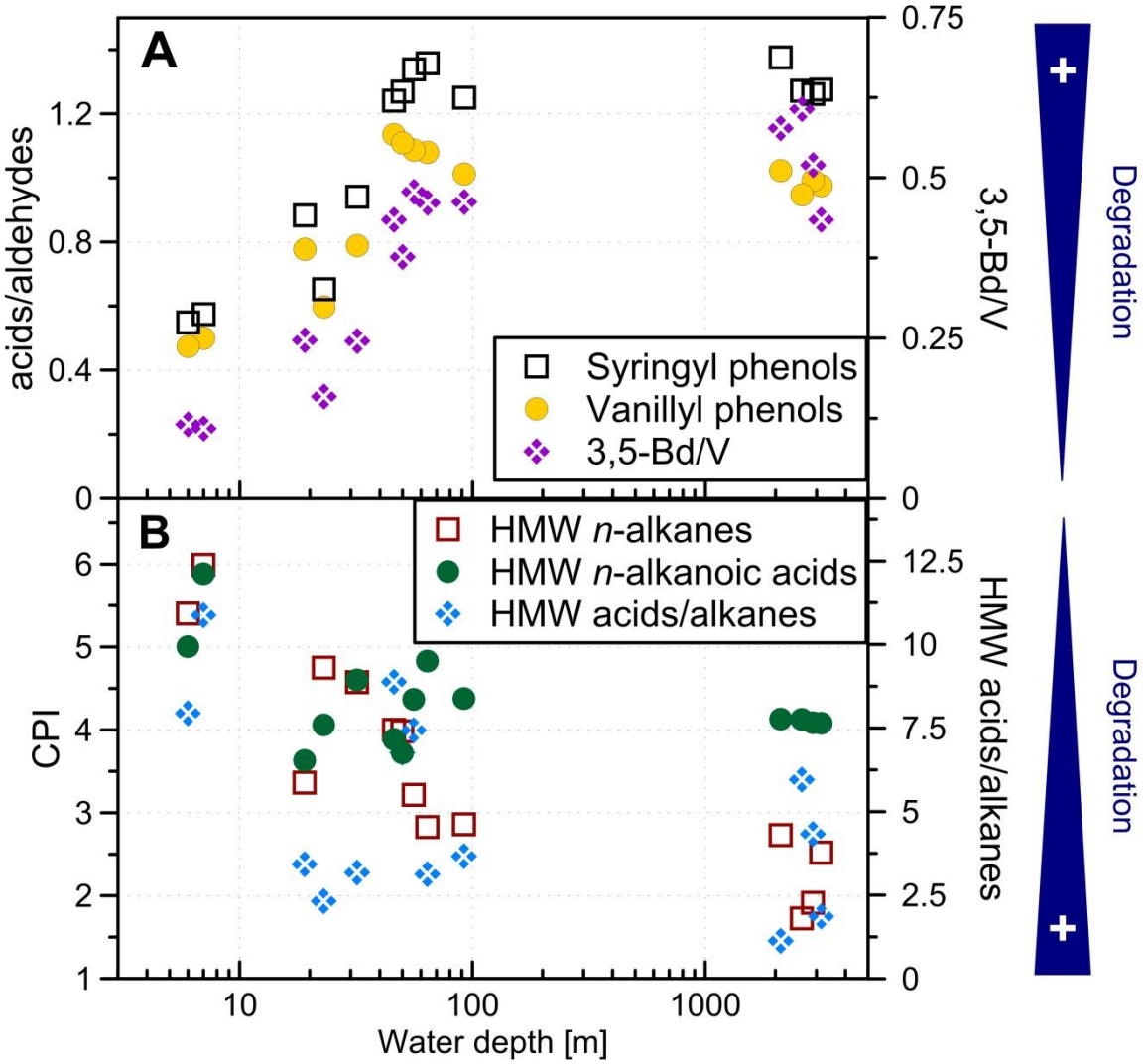


978

979 Figure 6: Degradation proxies for TerrOC, blue triangles point toward lower extent of
980 degradation: (A) CuO-oxidation derived ratios Sd/Sl, Vd/Vl and 3,5-Bd/V. (B) Carbon
981 preference indices (CPI) of HMW *n*-alkanes and *n*-alkanoic acidsand the ratio of HMW *n*-
982 alkanoic acids to HMW *n*-alkanes.

983

984 **Table 1: List of surface sediment samples from the Laptev Sea transect**

| ID | Sample type | Lat | Long | Water depth | OC | SA | $\delta^{13}C$ | $\Delta^{14}C$ | $SiO_2$ | $Al_2O_3$ | CaO |
|---|---|---|---|---|---|---|---|---|---|---|---|
| | | ° N | ° E | m | mg $g^{-1}$ | $m^2$ $g^{-1}$ | ‰ | ‰ | wt % | wt % | wt % |
| SW-1 | 0-0.5cm | 78.942 | 125.243 | 3146 | 10.4 | 34.0 | -22.34 | -418 | 60.3 | 16.5 | 2.4 |
| SW-2 | 0-0.5cm | 78.581 | 125.607 | 2900 | 13.8 | 38.3 | -22.70 | -392 | 57.8 | 17.2 | 2.1 |
| SW-3 | 0-0.5cm | 78.238 | 126.150 | 2601 | 10.6 | 31.8 | -22.61 | -426 | 62.1 | 16.0 | 1.6 |
| SW-4 | 0-0.5cm | 77.855 | 126.664 | 2106 | 13.2 | 41.5 | -22.51 | -428 | 56.6 | 17.5 | 1.3 |
| SW-6 | 0-1cm | 77.142 | 127.378 | 92 | 7.6 | 14.9 | -23.20 | -364 | 72.0 | 12.6 | 1.7 |
| SW-14 | 0-1cm | 76.894 | 127.798 | 64 | 8.9 | 19.4 | -24.33 | -314 | 71.3 | 12.5 | 1.5 |
| SW-23 | 0-1cm | 76.171 | 129.333 | 56 | 15.8 | 21.7 | -24.96 | -333 | 68.9 | 13.6 | 1.4 |
| YS-4 | 0-1cm | 75.987 | 129.984 | 50 | 13.4[a] | 31.4 | -24.76[a] | -284[a] | 63.8 | 15.1 | 1.3 |
| SW-24 | 0-1cm | 75.599 | 129.558 | 46 | 10.7 | 37.0 | -24.30 | -437 | 62.5 | 15.4 | 1.2 |
| YS-6 | 0-1cm | 74.724 | 130.016 | 32 | 18.6[a] | 31.6 | -25.60[a] | -465[a] | 62.1 | 16.1 | 1.3 |
| YS-9 | Grab | 73.366 | 129.997 | 23 | 13.1[b] | 16.9 | -26.10[b] | -415[b] | 70.8 | 14.0 | 1.3 |
| YS-13 | 0-1cm | 71.968 | 131.701 | 19 | 18.9[a] | 23.5 | -25.90[a] | -543[a] | 61.6 | 17.4 | 0.8 |
| YS-14 | 0-1cm | 71.630 | 130.050 | 7 | 19.1[a] | 11.4 | -26.20[a] | -504[a] | 69.6 | 15.0 | 1.6 |
| TB-46 | Grab | 72.700 | 130.180 | 6 | 25.8[a] | 12.0[c] | -26.50[a] | -436[a] | 67.9 | 15.2 | 1.8 |

985

986 [a] Data from Vonk et al. (2012); [b] data from Tesi et al. (2016); [c] data from Karlsson et al.
987 (2014).

988 **Table 2: Biomarker results for surface sediment samples from the Laptev Sea transect**

| ID | Lignin | Cutin | HMW* alkanes | HMW** acids | S/V | C/V | Sd/Sl | Vd/Vl | 3,5Bd/V | CPI alk | CPI acids | acids/ alk |
|---|---|---|---|---|---|---|---|---|---|---|---|---|
| | µg $m^{-2}$ | µg $m^{-2}$ | µg $m^{-2}$ | µg $m^{-2}$ | | | | | | | | |
| SW-1 | 0.56 | 0.063 | 0.14 | 0.27 | 1.1 | 0.09 | 1.3 | 0.98 | 0.43 | 2.5 | 4.1 | 1.9 |
| SW-2 | 0.41 | 0.070 | 0.13 | 0.57 | 0.99 | 0.16 | 1.3 | 0.99 | 0.52 | 1.9 | 4.1 | 4.3 |
| SW-3 | 0.34 | 0.061 | 0.13 | 0.75 | 0.92 | 0.14 | 1.3 | 0.95 | 0.61 | 1.7 | 4.1 | 6.0 |
| SW-4 | 0.42 | 0.048 | 0.093 | 0.10 | 1.1 | 0.08 | 1.4 | 1.0 | 0.58 | 2.7 | 4.1 | 1.1 |
| SW-6 | 0.68 | 0.12 | 0.18 | 0.67 | 0.90 | 0.19 | 1.2 | 1.0 | 0.46 | 2.9 | 4.4 | 3.7 |
| SW-14 | 1.0 | 0.12 | 0.15 | 0.46 | 1.0 | 0.08 | 1.4 | 1.1 | 0.46 | 2.8 | 4.8 | 3.1 |
| SW-23 | 0.97 | 0.17 | 0.16 | 1.2 | 0.96 | 0.11 | 1.3 | 1.1 | 0.48 | 3.2 | 4.4 | 7.4 |
| YS-4 | 0.84 | 0.17 | 0.13 | 0.92 | 0.83 | 0.17 | 1.3 | 1.1 | 0.38 | 4.0 | 3.7 | 6.8 |
| SW-24 | 0.76 | 0.23 | 0.18 | 1.6 | 0.84 | 0.19 | 1.2 | 1.1 | 0.43 | 4.0 | 3.9 | 8.9 |
| YS-6 | 2.7 | 0.71 | 0.31 | 0.97 | 0.68 | 0.27 | 0.94 | 0.79 | 0.25 | 4.6 | 4.6 | 3.2 |
| YS-9 | 10 | 2.7 | 0.45 | 1.1 | 0.60 | 0.31 | 0.65 | 0.60 | 0.16 | 4.7 | 4.1 | 2.3 |
| YS-13 | 5.8 | 2.3 | 0.64 | 2.3 | 0.65 | 0.29 | 0.88 | 0.78 | 0.25 | 3.4 | 3.6 | 3.4 |
| YS-14 | 34 | 9.0 | 1.1 | 12 | 0.66 | 0.42 | 0.57 | 0.50 | 0.11 | 6.0 | 5.9 | 11 |
| TB-46 | 45 | 11 | 0.83[d] | 6.6[d] | 0.64 | 0.53 | 0.55 | 0.47 | 0.12 | 5.4[d] | 5.0[d] | 7.9[d] |

989

990 * carbon chain-lengths 23-34; ** carbon chain-lengths 24-30.

991 [d] recalculated data from Karlsson et al. (2011).